PERGAMON

Progress in Biophysics & Molecular Biology 70 (1998) 95–136

Progress in Biophysics & Molecular Biology

The structure of iron–sulfur proteins

Heinrich Sticht *, Paul Rösch

Lehrstuhl für Struktur und Chemie der Biopolymere, Universität Bayreuth, Universitätsstr. 30, 95447 Bayreuth, Germany

Abstract

Ferredoxins are a group of iron–sulfur proteins for which a wealth of structural and mutational data have recently become available. Previously unknown structures of ferredoxins which are adapted to halophilic, acidophilic or hyperthermophilic environments and new cysteine patterns for cluster ligation and non-cysteine cluster ligation have been described. Site-directed mutagenesis experiments have given insight into factors that influence the geometry, stability, redox potential, electronic properties and electron-transfer reactivity of iron–sulfur clusters. © 1998 Elsevier Science Ltd. All rights reserved.

Keywords: Iron–sulfur proteins; Ferredoxins; HiPIPs; Structure; Mutational studies; Stability

1. Introduction

Iron–sulfur proteins are found in all organisms from 'primitive' archaea and bacteria to higher plants and animals. They are characterized by one or more non-heme iron ions ligated to inorganic sulfur and/or cysteine sulfur. These iron–sulfur clusters are components of electron transfer proteins, act as catalytic centers and function as sensors of iron and oxygen. They play a role in a variety of processes such as hydrogen metabolism, fixation of nitrogen or carbon monoxide, oxygenic phosphorylation, dehydration, mitochondrial hydroxylation and the reduction of nitrite and sulfite. The ubiquitous occurrence of iron–sulfur proteins and their presence in ancient organisms led to the hypothesis that these proteins have evolved during the very early stages of evolution.

A first subdivision of iron–sulfur proteins is possible into ferredoxins and rubredoxins, which contain exclusively iron–sulfur centers, and into complex iron–sulfur proteins, which contain prosthetic groups, such as flavine and heme, or other metals in addition to the iron–sulfur

* Corresponding author. Tel: +49-921-553-542; fax: +49-921-553-544; e-mail: heinrich.sticht@uni-bayreuth.de

0079-6107/98/$19.00 © 1998 Elsevier Science Ltd. All rights reserved.
PII: S0079-6107(98)00027-3

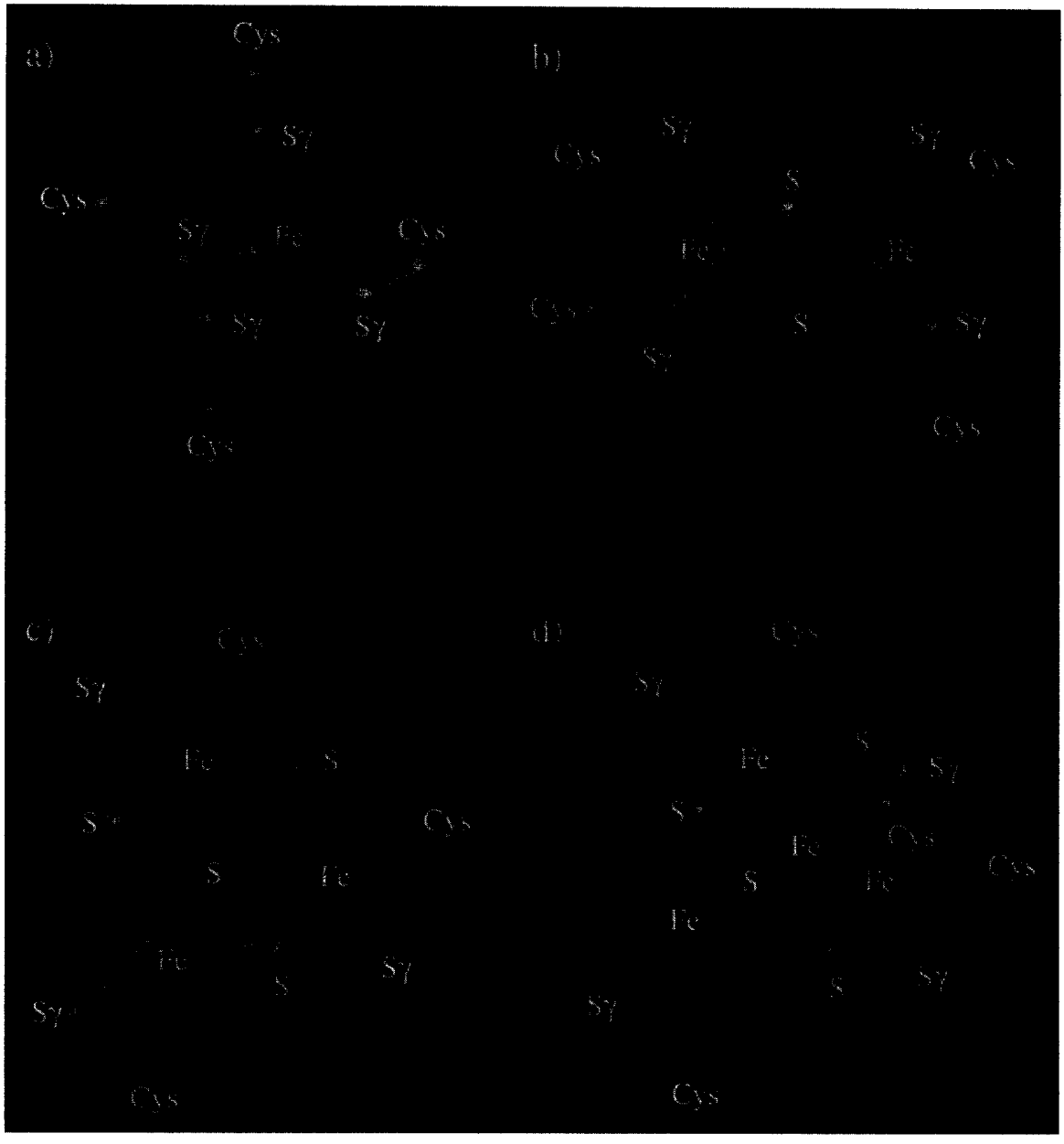

Fig. 1. Schematic representation of the four basic types of iron–sulfur clusters. The rubredoxin-type and the [2Fe–2S], [3Fe–4S] and [4Fe–4S] clusters are shown in (a) to (d), respectively.

centers. Ferredoxins and rubredoxins show electron transfer activity, but no classical enzymatic function, while the complex iron–sulfur proteins function in enzymatic catalysis rather than in electron transfer. The latter class of proteins has been the subject of recent reviews (Buckel, 1992; Beinert and Kennedy, 1993; Rouault and Klausner, 1996; Schäfer et al., 1996; Kisker et al., 1997) and will therefore not be discussed here.

The four types of structurally characterized iron–sulfur centers (Fig. 1) can be distinguished by the number of iron and inorganic sulfur atoms as: [1Fe], [2Fe–2S], [3Fe–4S] and [4Fe–4S]. Variations from cysteine ligation are known for several proteins, including oxygen ligation in aconitase or histidine ligation in Rieske centers.

The rubredoxin-type center contains one single high-spin Fe^{3+} or Fe^{2+} ion in the oxidized and reduced state, respectively. The [2Fe–2S] clusters of ferredoxins can exist in an oxidized state in which both high-spin Fe^{3+} ions are antiferromagnetically coupled and a reduced state with one Fe^{2+} and one Fe^{3+} atom. [3Fe–4S] clusters cycle between an oxidized form containing $3Fe^{3+}$ ions and a reduced form in which one of the iron ions is in the Fe^{2+} state. For the [4Fe–4S] clusters three different redox states are accessible: an oxidized state C^{+} ($3Fe^{3+}$, $1Fe^{2+}$), an intermediate state C^{0} ($2Fe^{3+}$, $2Fe^{2+}$) and a reduced state C^{-} ($1Fe^{3+}$, $3Fe^{2+}$). Only two of these states, however, are actually accessible as the oxidized and reduced states, depending on the type of [4Fe–4S] protein. C^{+} and C^{0} correspond to the oxidized and reduced form, respectively, of the high potential iron–sulfur proteins (HiPIPs), while the [4Fe–4S] ferredoxins exist either in the C^{0} or the C^{-} form (Carter et al., 1972).

Earlier work on ferredoxins has been reviewed in detail elsewhere (Bruschi and Guerlesquin, 1988; Meyer and Cusanovich, 1989; Beinert, 1990; Matsubara and Saeki, 1992) so that we can focus here on ferredoxins and related proteins for which new structural or mutational data has recently been reported.

Ferredoxin was first isolated in 1962 from the non-photosynthetic anaerobic bacterium *Clostridium pasteurianum* and was found to be involved in nitrogen fixation (Mortenson et al., 1962). A second ferredoxin was isolated immediately afterwards from spinach chloroplasts and was shown to function in photoreduction of $NADP^{+}$ (Tagawa and Arnon, 1962).

In subsequent years numerous novel ferredoxins were purified and investigations were aimed towards structure elucidation of these proteins and of their active sites. These studies have shown that the structural and functional diversity of ferredoxins is actually far greater than suggested by the small number of different cluster types, revealing an important role of the peptide moiety in modulating the properties of the cluster.

During recent years, the field of iron–sulfur proteins has been dramatically expanding due to the development of more sophisticated methods both in the field of molecular biology and structural biology, which allow rapid gene isolation and sequencing, the effective production of the necessary amount of protein for structural investigations and the design of site specific mutants. Site directed mutagenesis in conjunction with structure determination by NMR spectroscopy or X-ray crystallography continues to reveal important information about residues which are important for cluster formation, protein stability and for governing the electron transfer to and from other redox partners.

2. Ferredoxins containing [2Fe–2S] clusters

According to a previous classification by Matsubara and Saeki (1992) the [2Fe–2S] ferredoxins will be divided in this review into ferredoxins from oxygenic photosynthetic organisms and a structurally more distinct group of ferredoxins which are involved in various processes other than photosynthesis. The latter group includes the structurally characterized

Table 1
Sequence alignment of plant-type ferredoxins

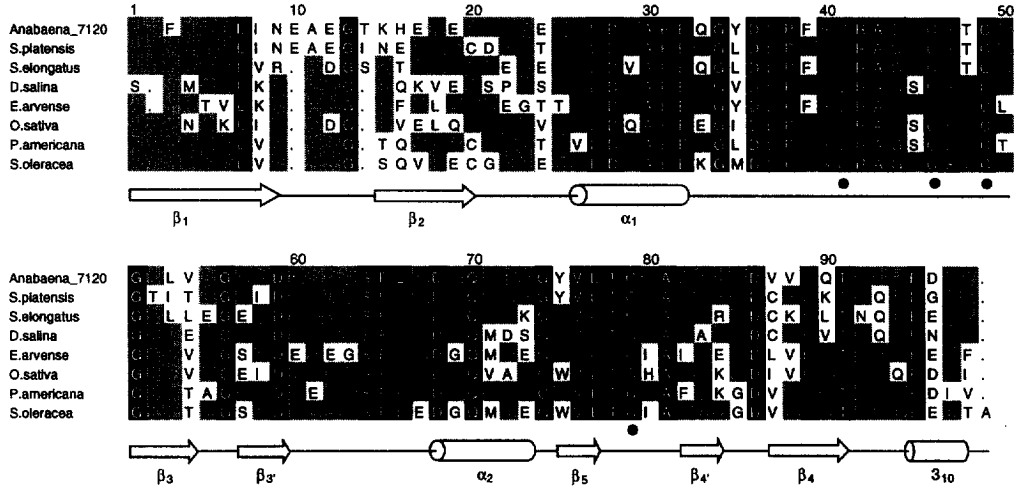

Sequence alignment of [2Fe–2S]-ferredoxins from blue–green algae (*Anabaena 7120* (Alam et al., 1986), *Spirulina platensis* (Tanaka et al., 1976) and *Synechococcus elongatus* (Baumann et al., 1996)), a green alga (*Dunaliella salina*, Hase et al., 1980) and plants (*Equisetum arvense* (Hase et al., 1977a), *Oryza sativa* (Kamo et al., 1989), *Phytolacca americana* (Wakabayashi et al., 1978) and *Spinacia oleracea* (Takahashi et al., 1983)).
The *Anabaena* 7120 numbering scheme is given at the top. The four cluster ligating cysteines are indicated by black circles (•). Strictly conserved residues at one position are highlighted by a black box and residues occurring with a frequency of ≥50% are marked by gray boxes. Common elements of secondary structure are given below the alignment.
The alignment was generated using the programs ClustalW (Higgins et al., 1992) and Alscript (Barton, 1993).

halobacterial ferredoxins, the ferredoxins from *Rhodobacter* and *Clostridium* and those present in oxygenase systems. The aldehyde oxido-reductase from *Desulfovibrio gigas*, for which a new [2Fe–2S] cluster-ligating motif has been reported, will be considered separately.

2.1. Ferredoxins involved in oxygenic photosynthesis

[2Fe–2S] ferredoxins involved in oxygenic photosynthesis act as terminal electron acceptor from photosystem I in green plant, algal and cyanobacterial photosynthesis. After one electron reduction of its [2Fe–2S] center, the ferredoxin reduces the FAD center of ferredoxin–$NADP^+$ reductase (FNR) in two one electron transfer steps resulting in the formation of NADPH (Masaki et al., 1982). In addition to oxygenic photosynthesis, chloroplast ferredoxins function in various ferredoxin-dependent reactions such as the reduction of nitrite to ammonia (Ida, 1977), nitrogen fixation (Schrautemeier and Böhme, 1985), glutamate synthesis (Lea and Miflin, 1984), sulfur assimilation (Aketagawa and Tamura, 1980), thioredoxin oxidoreduction (de Pascalis et al., 1993) and lipid desaturation (Schmidt and Heinz, 1990).

[2Fe–2S] ferredoxins show low redox potentials between −305 and −455 mV (Cammack et al., 1977a) and a very acidic p*I* of approximately 3 to 4.

2.1.1. Structure

Although the earliest cyanobacteria capable of oxygen-evolving photosynthesis appeared more than 3 billion years ago, the structures of the algal and plant ferredoxins are remarkably similar (Matsubara and Hase, 1983; Meyer, 1988) showing the highest degree of similarity for the residues flanking the cluster binding cysteines (Table 1). The sequences of these so-called plant-type ferredoxins contain 93 to 99 residues, corresponding to a molecular mass of approximately 11 kDa.

The crystal structures of four [2Fe–2S] ferredoxins from different organisms are known: *Spirulina platensis* (Fukuyama et al., 1980, 1995; Tsukihara et al., 1981), *Aphanothece sacrum* (Tsutsui et al., 1983; Tsukihara et al., 1990), *Anabaena* 7120 (Rypniewski et al., 1991; Jacobson et al., 1993) and *Equisetum arvense* (Ikemizu et al., 1994). For *Anabaena* 7120, the crystal structure of the heterocyst ferredoxin (Jacobson et al., 1993) is known in addition to the structure of the vegetative ferredoxin from the same organism (Rypniewski et al., 1991).

The solution structures of the cyanobacterial ferredoxins from *Synechocystis* sp. 6803 (Lelong et al., 1995) and from the thermophilic *Synechococcus elongatus* (Baumann et al., 1996) have been determined by a combined approach of NMR spectroscopy and molecular modeling, the latter one also by a modeling approach based on X-ray data from *Anabaena* Fd and some NMR-based restraints (Hatanaka et al., 1997). Detailed NMR studies were also carried out on the vegetative and heterocyst ferredoxin from *Anabaena* 7120 (Oh and Markley, 1990a,b; Oh et al., 1990; Chae et al., 1994).

As already expected from the high degree of sequence identity, all known three-dimensional structures are strikingly similar, showing pairwise C_α backbone rmsd values of approximately 1.0 Å. The major elements of secondary structure are two α-helices and a four stranded mixed β-sheet (Fig. 2a). Strands β_1 and β_2, which are connected by a hairpin loop, are running antiparallel, strand β_1 and β_4 running parallel and β_4 and β_3 running antiparallel to each other. Additional short β-strands were reported in the vicinity of strands β_3 and β_4 (denoted β_3' and β_4') and for residues 75–77 (strand β_5).

The loop connecting strands β_1 and β_2 frequently lacks two amino acids in the ferredoxins of higher plants, such as *E. arvense*, relative to those ferredoxins from the cyanobacteria *Anabaena* or *S. platensis* (Table 1). Ferredoxins with deletions of these two amino acids always have a proline at position 11, defining a turn rather than a loop between the strands of β-sheet (Tsukihara et al., 1990).

The different ferredoxin structures vary in the number of the short β-sheets and in the absence of the second α-helix (α_2) in *A. sacrum* Fd (Tsukihara et al., 1990). These differences are most likely due to the accuracy of the X-ray structures, generally showing resolutions of less than 2.0 Å as well as poor electron densities and high temperature factors in the corresponding sequence regions. This assumption was confirmed recently by the refinement of the *S. platensis* Fd structure, establishing the presence of the second α-helix in this protein that was missing in earlier studies (Fukuyama et al., 1995).

The tertiary structure of each ferredoxin is mainly defined by a hydrophobic core and the [2Fe–2S] cluster. The hydrophobic core is formed by several conserved amino acids and is

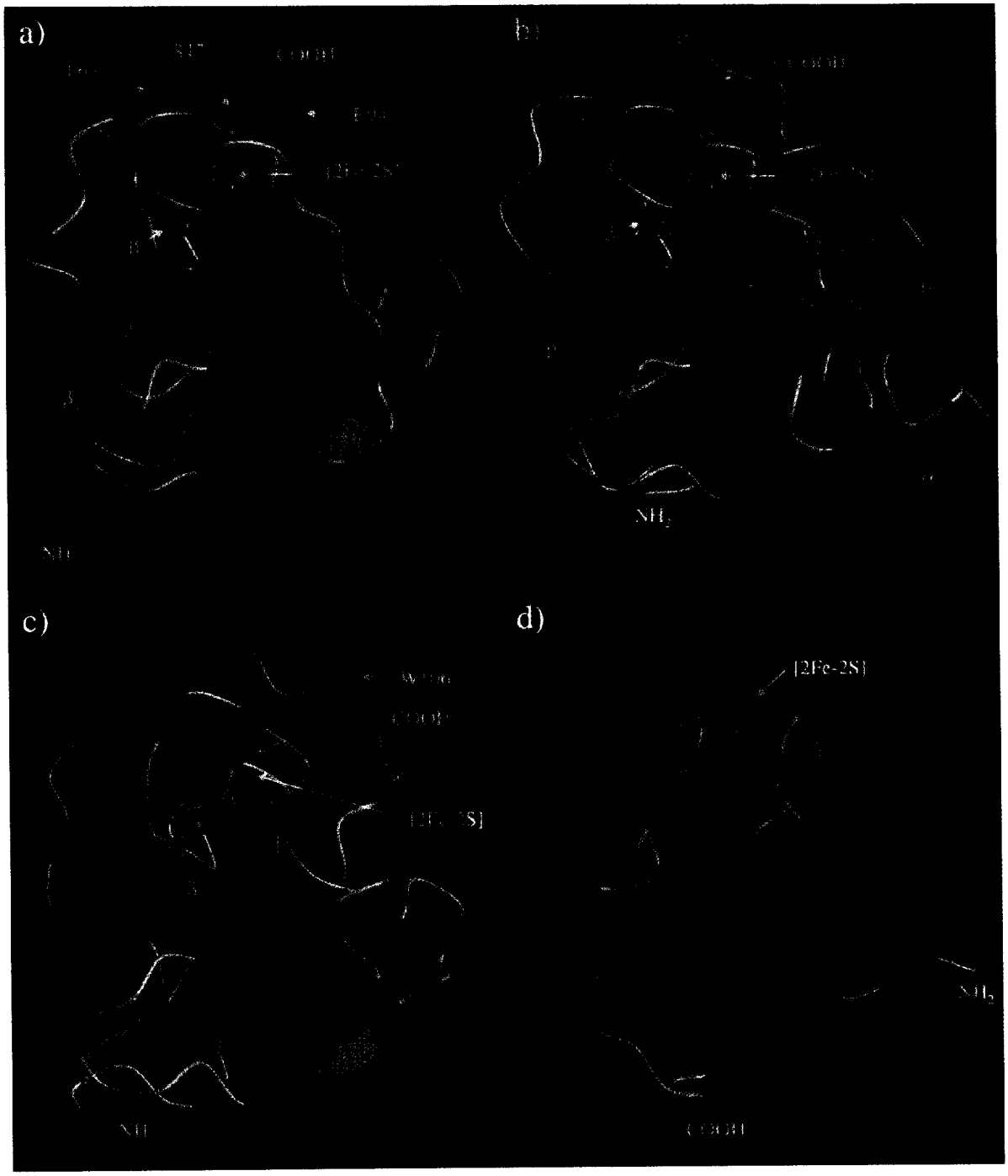

Fig. 2. Schematic ribbon representation of the three-dimensional structures of various [2Fe–2S] cluster containing proteins: Elements of regular secondary structure are indicated and labeled according to the nomenclature in Tables 1 and 2. The [2Fe–2S] clusters, their ligating cysteines and other functionally important residues are shown in ball-and-stick presentation. All figures were generated using the programs MOLSCRIPT (Kraulis, 1991) and

more extended in the ferredoxin from the thermophilic *S. elongatus* (Baumann et al., 1996; Hatanaka et al., 1997). The iron sulfur cluster is located in a loop segment towards the outer edge of the molecule, near the protein surface and approximately 10 Å from the hydrophobic core. The geometry of the cluster and of the peptide chain, which adopts ϕ and ψ angles not typical for elements of regular secondary structure, is strictly conserved among all ferredoxins. The cluster consists of two irons, each of them tetrahedrally coordinated by two inorganic sulfurs and by sulfurs of two cysteine residues. One iron atom is coordinated by the Sγ atoms of Cys41 and Cys46, the other by those of Cys49 and Cys79. These four covalent bonds were suggested to play a significant role in maintaining the three-dimensional structure of this surface loop (Holden et al., 1994).

In addition, this region is stabilized by numerous hydrogen bonds and one salt bridge between the highly conserved residues Arg42 and Glu31 (Matsubara and Hase, 1983). The pattern of these interactions is very similar for all ferredoxins, including a network of hydrogen bonds that connects the cluster binding region with the C-terminal helix and with the loop around Ser64 (Holden et al., 1994). Analysis of the crystal structures also revealed eight conserved hydrogen bonds to the cluster; five of them between backbone amide hydrogens and Sγ atoms of the cysteine ligands and three between backbone amide hydrogens and the inorganic sulfurs of the cluster.

Correlation of the length and pattern of the hydrogen bonds with the redox potentials is difficult at the present resolution of less than 2.0 Å for most of the structures, but the overall similarities suggest that their role in modulating the redox potential might be less important than previously suggested (Backes et al., 1991).

Unique structural elements that have been related to the increased thermostability of *S. elongatus* Fd are an extended hydrophobic core, a hydrophobic patch at the protein surface and a more extended network of electrostatic interactions mainly between the side chains of charged amino acids (Baumann et al., 1996; Hatanaka et al., 1997).

2.1.2. Mutational studies

Up to now, over 50 mutants of *Anabaena* 7120 vegetative Fd have been designed to investigate cluster assembly and stabilization and to determine which residues are important for recognition and electron transfer to its redox partners (Holden et al., 1994). In addition, X-ray crystallographic structure determinations have been carried out for seven of these mutants (Hurley et al., 1997a,b).

Raster3D (Bacon and Anderson, 1988; Merritt and Murphy, 1994). (a) Structure of *Anabaena* 7120 vegetative ferredoxin (Rypniewski et al., 1991). Residues Ser47, Phe65 and Glu94, which play a crucial role for the interaction with FNR are shown in ball-and-stick representation. (b) Structure of the [2Fe–2S] ferredoxin from *Haloarcula marismortui* (Frolow et al., 1996). In order to facilitate the comparison, the same orientation as in (a) is shown. The N-terminal extension, that is not present in plant-type ferredoxins, includes the helices α′ and α″ and their connecting turn. (c) Structure of putidaredoxin from *Pseudomonas putida* (Pochapsky et al., 1994a). Trp106, which is involved in the interaction with $P\text{-}450_{cam}$ is shown in ball-and-stick presentation. In order to facilitate the comparison, the same orientation as in (a) is shown. (d) Structure of the second [2Fe–2S] cluster binding domain of the aldehyde oxidoreductase from *D. gigas*, which shows a completely different cluster ligating motif (Romao et al., 1995).

Interactions of native and mutant *Anabaena* Fd were studied by laser flash photolysis measuring the kinetics of reduction of oxidized Fd by deazariboflavin semiquinone and the reduction of oxidized ferredoxin–$NADP^+$-reductase (FNR) by oxidized Fd (Hurley et al., 1993a, 1996a,b). None of the mutations designed for residues Arg42, Ser47, Thr48, Asp62, Ser64, Phe65, Asp68, Asp69, Gln70, Glu94 and Glu95 influenced the second-order rate constant for deazariboflavin semiquinone reduction significantly, suggesting that all mutants were still capable of participating in electron transfer (Holden et al., 1994; Hurley et al., 1997a).

For the surface charge reversal mutant E94K and for the double mutant E94K/E95K a decrease in the electron transfer rate from Fd to FNR by more than 3 orders of magnitude was reported, while no changes were observed for the single substitution of the adjacent residue E95K (Hurley et al., 1993a).

A decreased rate constant for the Fd–FNR electron transfer was observed for mutations of Phe65 to Ile or Ala, but not for replacements by Trp of Tyr, showing the requirement of an aromatic amino acid at sequence position 65 for efficient electron transfer (Fig. 2a). Interestingly, a double mutant (S64Y/F65A), in which an aromatic amino acid is introduced adjacent to the position in the wild-type protein, shows similar characteristics as the F65A mutant and fails to restore the electron transfer activity of the native protein (Hurley et al., 1993a,b).

Recently, a third kinetically inactive mutant (S47A) has been described, revealing the importance of a hydrogen bond which exists between the hydroxyl group of Ser47 and the side-chain carboxyl group of Glu94. This finding is confirmed by the properties of a S47T mutant, which restores wild-type electron-transfer activity (Hurley et al., 1997a).

The fact that several mutations in the vicinity of Glu94, Phe65 and Ser47 (Arg42, Thr48, Ser64, Glu95) did not perturb the Fd–FNR interaction led to the proposal of a high degree of localization and specificity in the electron-transfer region of the two proteins (Hurley et al., 1993a; Gómez-Moreno et al., 1994).

Measurement of the redox potential of mutant ferredoxins revealed that those amino acids which are critical for the Fd–FNR electron-transfer process also play a disproportionally large role in determining the redox potential of the [2Fe–2S] cluster. Large positive shifts of the reduction potential up to +93 mV were measured for the kinetically inactive mutants E94K, E94Q, F65A, F65I and S47A, while the redox potential of the other mutants is much more similar to that of the wild-type ferredoxin (Hurley et al., 1997a).

Despite this strong correlation between positive potential shifts and a decrease in electron transfer reactivity, it was proposed that reduction potential changes are not the principal factor governing electron-transfer reactivity. This conclusion is mainly based on the observation that all three kinetically inactive ferredoxin mutants induce large positive shifts (~40 mV) of the FNR reduction potential after complex formation with recombinant FNR. This behavior, which is also observed for the wild-type ferredoxin, renders the electron transfer in the physiological direction isopotential (for E94K) or thermodynamically favorable (for F65I and S47A), thereby overcoming the unfavorable positive potential shifts observed for the free ferredoxin mutants. This finding implies large parallel effects of the mutation of the three critical residues (Ser47, Phe65, Glu94) on both the reduction potential and the electron-transfer reactivity of the [2Fe–2S] cluster, suggesting that the principal determinant of electron-transfer

reactivity is the orientation of the redox partners within the transient protein–protein complex (Hurley et al., 1997a).

Structure determination of the D62K, D68K, E94K, E95K, Q70K and S47A mutants revealed that none of these mutants exhibits significant structural changes in the immediate vicinity of the [2Fe–2S] cluster, indicating that large decreases in electron transfer reactivity and the significant increases in reduction potential, which were observed for the E94K and S47A mutant, do not result from gross structural changes (Hurley et al., 1997a). These findings are in agreement with previous studies which proved that all mutants investigated showed binding constants to FNR similar to the wild-type ferredoxin (Hurley et al., 1993a)

All these points strongly support the hypothesis that even kinetically inactive mutants are still capable of forming tight complexes with FNR and of inducing thermodynamically favorable changes in its redox properties. The presence of nonproductive complexes after mutation of the critical residues (Ser47, Phe65, Glu94) was attributed to a perturbation of the normal docking interactions leading to slightly different orientations of the redox partners in the Fd–FNR complex (Hurley et al., 1997a).

Additional studies have revealed that nonconservative mutations of Phe65 or Glu94, which were previously shown to result in large decreases of the electron transfer to FNR (Holden et al., 1994), exhibited wild-type behavior in their reaction with photosystem I (Navarro et al., 1995). It was concluded that different sites have evolved independently for interactions with the different redox partners, FNR and photosystem I.

UV-vis, NMR and EPR spectroscopic characterization of four mutants in which the four cluster ligating cysteines were individually changed to serines, proved the spectroscopic properties of each of the mutants to be different from the wild-type (Cheng et al., 1994). In spite of these differences, the crystal structure of the C49S mutant is virtually identical to that of the wild-type ferredoxin, showing that serine is able to replace cysteine as a cluster ligand (Hurley et al., 1997b). The cysteine mutants C41S, C46S and C49S are still capable of participating in the electron transfer reaction, suggesting that cysteine sulfur d-orbitals are not essential for electron transfer (Hurley et al., 1997b). The exclusive occurrence of cysteine as native cluster ligand was explained by the difference in pK_a between serine and cysteine, resulting in higher stability for cysteine ligation (Cheng et al., 1994).

Mutation of residue Glu92 of spinach ferredoxin to lysine, glutamine or alanine shifted the potential positively by 93, 73 and 78 mV, respectively (Aliverti et al., 1995). Both direction and magnitude of these potential shifts are similar to those reported for mutations of the analogous residue (Glu94) in *Anabaena* Fd (Hurley et al., 1997a). In the spinach system, however, only a moderate decrease of the electron transfer rates was detected for the Glu92 mutants and this was mainly attributed to the shifts of the redox potential observed after substitution of Glu92 (Piubelli et al., 1996).

A comparison of the electron-transfer reactivity between the *Anabaena* and spinach ferredoxins, however, proves to be difficult, since different reactions were measured in both systems utilizing flash laser spectroscopy and cytochrome c reduction, respectively (Piubelli et al., 1996; Hurley et al., 1997a). Therefore, it appears not yet totally clear whether different rate-limiting steps have been measured in both systems or whether species differences account for the discrepancies observed.

2.1.3. Anabaena 7120 heterocyst ferredoxin

Many organisms have several isoforms of [2Fe–2S] ferredoxins, which are believed to have evolved by gene duplication that occurred long before functional specification (Matsubara et al., 1978, 1980; Matsubara and Hase, 1983). Although some ferredoxin isoforms differ considerably in their amino acid sequences and their redox potentials (Hutson and Rogers, 1975; Cammack et al., 1977a; Hase et al., 1982), a functional distinction proved to be difficult on the basis of the enzymatic assay systems currently used (Matsubara and Saeki, 1992).

An excellent and comprehensive overview of the different functions and biochemical properties of ferredoxin isoforms is given by Matsubara and Saeki (1992). We will focus here on one special ferredoxin isoform from *Anabaena*, the so-called heterocyst ferredoxin, for which detailed structural and functional information is available.

Anabaena 7120 heterocyst ferredoxin is only found in cyanobacterial cells that have differentiated into nitrogen-fixing heterocysts. Like the vegetative ferredoxin (VFd), heterocyst ferredoxin (HFd) can function in photosynthetic electron transport. However, this ferredoxin has an additional unique function in nitrogen fixation by donating electrons to component II (the iron-protein) of nitrogenase (Schrautemeier and Böhme, 1985; Böhme and Schrautemeier, 1987b).

Although the vegetative and heterocyst ferredoxins show 51% sequence identity and are presumed to have evolved from a common ancestral gene, they differ in their midpoint redox potentials, immunological cross reactivities, isoelectric points, EPR and NMR spectra (Böhme and Schrautemeier, 1987a; Correll et al., 1992; Salamon and Tollin, 1992; Chae et al., 1994; Chae and Markley, 1995a).

Comparison of the crystal structures (Rypniewski et al., 1991; Jacobson et al., 1993) reveals that VFd and HFd have a very similar fold with an overall backbone rmsd less than 1 Å, suggesting that the functional differences of both proteins are due to subtle structural differences, presumably in the cluster vicinity. NMR studies have revealed that one major difference between the two proteins is in their dynamics, as evidenced by lower hydrogen exchange rates and higher helix stabilities observed for VFd (Chae et al., 1994; Holden et al., 1994). Four of the 22 amino acids thought to be strictly conserved in all vegetative ferredoxins are not retained in HFd (Matsubara and Hase, 1983). Three of these residues, His42, Ser43 and Leu78, are located near the iron–sulfur cluster. The other nonconserved residue in HFd is Ala76, which is typically a valine (Holden et al., 1994).

The replacement of Arg42 which is salt-bridged in VFd, by His42 in HFd, does not result in a rearrangement of the protein backbone, but was proposed to change both the flexibility of the polypeptide chain and the surface properties of the protein in that region (Jacobson et al., 1993). Thermodynamically, the HFd mutant H42R is more stable than the wild-type HFd by precisely the amount of stability lost in VFd upon substitution of Arg42 by His (Hurley et al., 1995).

The structural basis for the different physical and chemical properties of vegetative and heterocyst Fd was further investigated by swapping a minimal number of conserved residues from the sequence of one ferredoxin to the other (Chae and Markley, 1995b). Analysis of the UV-vis and NMR spectral properties revealed that the change from the VFd phenotype to the HFd phenotype can be achieved by single amino acid swapping (T78L) or by swapping a set of five other residues (R42H, A43S, A45S, T48S, A50V) in a very different part of the sequence.

In contrast, the reciprocal mutations of HFd were not sufficient to convert the spectral properties to those of VFd, revealing very discriminating sequence requirements in the more rigid VFd (Chae et al., 1994; Chae and Markley, 1995b).

2.2. Halobacterial ferredoxins

Two [2Fe–2S] ferredoxins with a molecular weight of 14–15 kDa were isolated from the extremely halophilic archaea *Halobacterium halobium (salinarium)* (Kerscher and Oesterhelt, 1976; Kerscher et al., 1976) and from *Haloarcula marismortui* (Werber and Mevarech, 1978a) where they are present in large amounts. Both ferredoxins do not function in the NADP-photoreduction system: *H. halobium* Fd was suggested to serve as an electron carrier in the decarboxylation of α-ketoacids (Kerscher and Oesterhelt, 1977), while *H. marismortui* Fd was reported to function in the dissimilatory reduction of nitrite (Werber and Mevarech, 1978b).

Halobacterial ferredoxins are homologous to plant-type ferredoxins but they are 30 residues longer and contain an extremely high excess of acidic amino acids (Werber and Mevarech, 1978a). The sequence similarity (identity) to other plant and cyanobacterial ferredoxins is approximately 50–70% (30–40%) (Pfeifer et al., 1993), while the sequence similarity between both halobacterial ferredoxins is 91% (Table 2). In contrast, no significant homology exists to known vertebrate ferredoxins. The UV-vis, CD- and EPR-spectra, as well as the location and spacing of cysteines in the amino acid sequence of halobacterial ferredoxins closely resemble the plant type ferredoxins, while the redox potential of −340 to −350 mV is slightly higher (Werber and Mevarech, 1978a). Both halobacterial ferredoxins contain a single acetylated lysine residue at position 118 with unknown biological significance (Hase et al., 1978).

The crystal structure of the [2Fe–2S] ferredoxin from *H. marismortui* was recently determined at a resolution of 1.9 Å (Frolow et al., 1996), giving insight into the structural principles of halophilic adaption (Fig. 2b). The structure can be divided into a core part (residues 39–128), which shows a fold similar to plant type ferredoxins and an extra N-terminal extension, consisting of two amphipathic helices (α′ and α″) and intervening loops (residues 6–38).

The sequence of the core domain shows approximately 35% identity to the sequences of plant-type ferredoxins. Exclusion of the C-terminal helix, which is not present in plant-type ferredoxins, results in backbone rmsd values of less than 1 Å between *H. marismortui* and *Anabaena* ferredoxin and the arrangement of the [2Fe–2S] cluster and its ligating cysteines is essentially the same in these two proteins.

The N-terminal α-helices α′ and α″ are inserted between strands β_1 and β_2 (Fig. 2b) in *H. marismortui* Fd, whereas in plant-type ferredoxins these two strands are connected by a short loop or turn. The N-terminal domain contains 15 negative and no positive charges, providing numerous surface carboxylates with high water binding capability, which was suggested to play a role in preventing the protein from self aggregation (Frolow et al., 1996).

The core domain is less acidic than the N-terminal domain and its six basic residues are involved in the formation of four salt-bridges. For the highly conserved Glu53–Arg64 salt bridge a functionally important role was proposed on the observation that this salt-bridge protects the iron sulfur cluster from access to the solvent. The halophilic adaption of this protein was mainly attributed to the extraordinary capability of the numerous carboxylates to

Table 2
Structure-based sequence alignment of halobacterial and plant-type ferredoxins

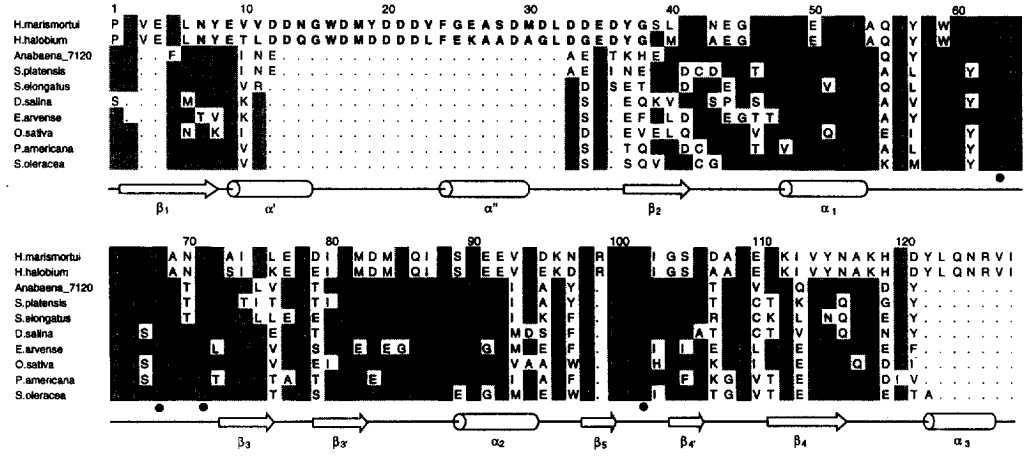

Sequence alignment of [2Fe–2S]-ferredoxins from two halobacteria (*Haloarcula marismortui* (Frolow et al., 1996) and *Halobacterium halobium* (Pfeifer et al., 1993)), blue–green algae (*Anabaena 7120* (Alam et al., 1986), *Spirulina platensis* (Tanaka et al., 1976) and *Synechococcus elongatus* (Baumann et al., 1996)), a green alga (*Dunaliella salina* (Hase et al., 1980)) and plants (*Equisetum arvense* (Hase et al., 1977a), *Oryza sativa* (Kamo et al., 1989), *Phytolacca americana* (Wakabayashi et al., 1978) and *Spinacia oleracea* (Takahashi et al., 1983)).
The *H. marismortui* numbering scheme is given at the top. The four cluster ligating cysteines are indicated by black circles (•). Strictly conserved residues at one position are highlighted by a black box and residues occurring with a frequency of ≥50% are marked by gray boxes. Elements of secondary structure present in the *H. marismortui* structure (Frolow et al., 1996) are given below the alignment. The N-terminal extension, that is not present in plant-type ferredoxins is marked by bold letters.
The alignment was generated using the programs ClustalW (Higgins et al., 1992) and Alscript (Barton, 1993).

bind water molecules and to the presence of six bound K^+ ions, shielding the protein from its environment (Frolow et al., 1996).

2.3. *Rhodobacter ferredoxins*

Rhodobacter capsulatus, a photosynthetic bacterium which is capable of fixing molecular nitrogen, contains at least six different ferredoxins (Jouanneau et al., 1995b). FdI and the homodimeric FdIII contain two [4Fe–4S] clusters per monomer (Jouanneau et al., 1993), while FdII was shown to bind one [3Fe–4S] and one [4Fe–4S] cluster (Jouanneau et al., 1990). FdIV, FdV and FdVI are representatives of the [2Fe–2S] ferredoxins, encoded by the genes *fdxC*, *fdxD* and *fdxE*, respectively (Grabau et al., 1991; Armengaud et al., 1994; Naud et al., 1994).

FdVI shows 42% sequence identity with putidaredoxin from *Pseudomonas putida* and was therefore suggested to transfer electrons to oxygenases, such as P-450 cytochromes (Naud et al., 1994).

FdIV and FdV both contain four conserved cysteines in a spacing characteristic of [2Fe–2S] plant-type ferredoxins, suggesting a cluster ligation pattern identical to that of plant-type ferredoxins. FdIV and FdV show a low sequence identity of 16% and a limited sequence identity of 15–25% compared to the plant-type ferredoxins (Armengaud et al., 1994).

FdIV was suggested to be involved in nitrogen fixation, since its gene is cotranscribed with the gene coding for FdI only under nitrogen-limited growth conditions (Grabau et al., 1991; Saeki et al., 1991). However, the exact physiological function of FdIV in nitrogen fixation still remains to be clarified.

FdV is inefficient as an electron donor for FNR in photoreduction which was attributed to its high redox potential (–220 mV) or to some structural features different from plant type ferredoxins. The functionally important residues Phe65 and Glu94 (Hurley et al., 1993a,b) that are strictly conserved among plant ferredoxins, are replaced by methionine and glycine, respectively, in *R. capsulatus* FdV (Armengaud et al., 1994).

FdV proved to be ineffective as electron donor for nitrogenase in vitro (Armengaud et al., 1994). Although FdV is not required for N_2 fixation, it may provide protection of nitrogenase against oxidative damage in analogy to *Azotobacter vinelandii* Fe–S protein II (Moshiri et al., 1994).

2.4. *Clostridium ferredoxin*

Clostridium pasteurianum [2Fe–2S] ferredoxin (Fd_{Cp}) consists of 102 amino acids including five cysteines at positions 11, 14, 24, 56 and 60 (Meyer et al., 1986; Meyer, 1993). Both the sequence and distribution of the cysteine residues are unique among [2Fe–2S] ferredoxins (Table 3) suggesting that there are several ferredoxin groups that originated from different ancestors (Bruschi and Guerlesquin, 1988; Meyer, 1988). In its native state the protein is a dimer containing one [2Fe–2S] cluster in each subunit. *C. pasteurianum* ferredoxin was recently shown to interact strongly and specifically with the MoFe protein of nitrogenase and three

Table 3
Distribution of the cluster-ligating cysteines in various groups of [2Fe–2S] cluster containing proteins

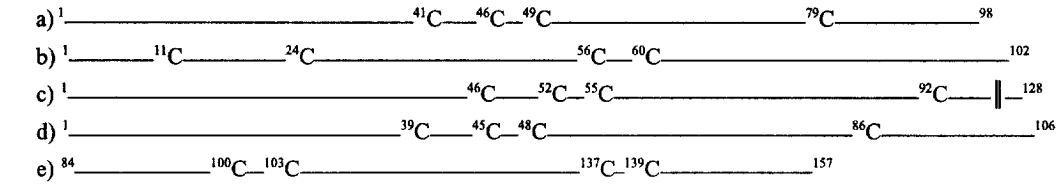

Cysteines, that ligate the [2Fe–2S] cluster are labeled with their sequence position. Schematic presentations of the peptide chain indicating the location of the cysteines are shown for (a) *Anabaena* 7120 [2Fe–2S] ferredoxin (Rypniewski et al., 1991), (b) *C. pasteurianum* [2Fe–2S] ferredoxin (Meyer et al., 1986), (c) bovine adrenodoxin (Miura et al., 1991), (d) *P. putida* [2Fe–2S] putidaredoxin (Pochapsky et al., 1994a,b) and (e) second [2Fe–2S] cluster binding domain of *D. gigas* aldehyde oxidoreductase (Romao et al., 1995).

glutamate residues (Glu31, 34, 38) of the ferredoxin proved to be important for this interaction (Golinelli et al., 1997).

All five cysteines have been mutated into serine or alanine providing the assignment of cysteines 11, 24, 56 and 60 as ligands of the cluster in the wild-type protein (Fujinaga et al., 1993; Meyer et al., 1994; Golinelli et al., 1996). The observation that the cluster is still assembled in the C24A variant was attributed to a ligand swapping in which Cys14 is promoted to become the fourth ligand (Golinelli et al., 1996). In a protein in which both Cys24 and Cys14 are mutated to alanine, a newly introduced cysteine at position 16 is able to serve as the fourth ligand of the cluster. Cys14 and Cys24 are located in a solvent-exposed flexible loop, in which up to 14 amino acids can be deleted without severely affecting stability and spectroscopic properties of the protein, as evidenced from UV-vis, resonance Raman, magnetic circular dichroism and EPR studies. The mutations, however, resulted in changes of the redox potential over a range of 100 mV (Golinelli et al., 1996).

Recent studies have shown that a double mutation of Cys14 and Cys24 to alanine did not prevent cluster assembly in this variant containing a total of only three cysteines. ^{14}N-ESEEM spectra of this variant were very similar to the wild-type protein, giving no evidence for a direct nitrogen coordination by histidine or any other ^{14}N nuclei. For an individual or collective replacement of the three histidines in Fd_{Cp} only marginal differences of the spectroscopic properties compared to the wild-type were reported, confirming that histidine is not the fourth ligand in the C14A/C24A double mutant and ruling out a 'rieske-type' cluster coordination (Shergill et al., 1996).

Since the three-dimensional structure of Fd_{Cp} is unknown, the nature of the fourth cluster ligand is not definitely known up to now. Possible candidates include methionine, serine, aspartate and glutamate residues or exogenous oxygenic ligands from the solvent such as H_2O/OH^- (Shergill et al., 1996).

2.5. Ferredoxins in oxygenase systems

A first rough division of this group of ferredoxins can be made into putidaredoxin from *Pseudomonas putida* and the vertebrate-type ferredoxins.

Vertebrate ferredoxins are small (13–14 kDa) single [2Fe–2S] proteins, which have been isolated from the mitochondria of various tissues including adrenocortex, ovary, thyroid, placenta, kidney, liver and brain (Ichikawa et al., 1987). They function to transfer electrons from NADPH-dependent ferredoxin reductase to the cytochrome P450 enzymes involved in the biogenesis of steroid hormones, the formation of vitamin D metabolites and the production of bile acids (Mason and Boyd, 1971; Simpson and Miller, 1978).

Vertebrate ferredoxins consist of 117–128 residues and contain five cysteines at positions 46, 52, 55, 92 and 95 (Table 3). Cys95 carries a free thiol group and the other four cysteines have been shown to function as ligands of the [2Fe–2S] cluster (Cupp and Vickery, 1988; Xia et al., 1996).

The redox potential of the vertebrate ferredoxins (~ -270 mV) is considerably higher than that of the plant-type ferredoxins (~ -400 mV) (Cammack et al., 1977a). These differences can be correlated with differences in the electronic structure of the iron–sulfur clusters between vertebrate ferredoxins and *Anabaena* ferredoxin, which have been detected by NMR

spectroscopic studies. While the ^1H hyperfine signals from oxidized vertebrate ferredoxins are similar to those of plant-type ferredoxins, significant differences exist between the reduced forms of plant and vertebrate ferredoxins, suggesting different patterns of electron delocalization in the reduced iron–sulfur clusters (Skjeldal et al., 1991).

NMR studies were also used to investigate the reasons for the pH dependence ($pH_{mid} = 7.2$) of the redox potential of vertebrate ferredoxins, an effect that is not observed for the plant-type ferredoxin from spinach (Cooper et al., 1973; Lambeth and Kamin, 1979). This behavior was previously attributed to the titration of the imidazole side-chain of a histidine, presumably to that of the conserved His56 which is adjacent to the cluster-ligating Cys55 (Lambeth et al., 1982; Greenfield et al., 1989).

This was, however, ruled out by a recent NMR study indicating that none of the three histidines (His10, 56, 62) interacts directly with the [2Fe–2S] cluster and that His56 does not titrate between pH 6.0 and 8.6 in either the oxidized or reduced form of human ferredoxin (Xia et al., 1995). According to the chemical shifts, His56 has a pK_a value of < 5 (Xia et al., 1995), which may result from solvent inaccessibility or from a strong hydrogen bond, possibly to Ser88 (Miura et al., 1991).

The 106-residue Putidaredoxin (Pdx) found in the bacterium *Pseudomonas putida* shows a sequence similarity of approximately 50% compared to the vertebrate ferredoxins. It contains a single [2Fe–2S] cluster and acts as an electron donor to Cytochrome $P\text{-}450_{cam}$, a monooxygenase which catalyzes the first step in camphor catabolism, the 5-*exo*-hydroxylation of camphor by molecular oxygen (Cushman et al., 1967).

The presence of Pdx is absolutely essential for the turnover of the ternary complex between reduced $P\text{-}450_{cam}$, O_2 and camphor, showing that Pdx plays an effector role for catalysis by $P\text{-}450_{cam}$. While $P\text{-}450_{cam}$ can also be reduced by other [2Fe–2S] proteins like adrenodoxin and spinach ferredoxin, these proteins proved to be incompetent for the effector role of Pdx (Lipscomb et al., 1976; Shiro et al., 1989; Ye et al., 1992).

The binding affinity for oxidized $P\text{-}450_{cam}$ is 100-fold higher for reduced Pdx compared to oxidized Pdx (Hintz et al., 1982) and $P\text{-}450_{cam}$ bound Pdx ($E_{obs} = -196$ mV) is more readily reduced than free Pdx ($E_{obs} = -230$ mV) (Sligar and Gunsalus, 1976). The C-terminal residue of Pdx, Trp106, was shown to be required for an effective binding to $P\text{-}450_{cam}$ and is transferred from aqueous solution to a nonpolar environment upon complex formation (Davies et al., 1990; Davies and Sligar, 1992).

The structure of Pdx, its redox-dependent dynamics and its interactions with $P\text{-}450_{cam}$ have been subject of numerous NMR spectroscopic and modeling studies (Ye et al., 1992; Ratnaswamy and Pochapsky, 1993; Pochapsky et al., 1994a,b; Kazanis et al., 1995; Lyons et al., 1996; Pochapsky et al., 1996; Kazanis and Pochapsky, 1997).

The structure of Pdx was determined by NMR spectroscopy (Fig. 2c), using additional structural restraints from model compounds and known ferredoxin structures for the cluster environment, which is underdetermined from NMR data as a consequence of paramagnetic line broadening (Ye et al., 1992; Pochapsky et al., 1994a).

Pdx shows significant structural homology to the plant-type [2Fe–2S] ferredoxins of known structure, including the four-stranded β-sheet and the first α-helix (Fig. 2a and c). Additional elements of secondary structure in Pdx include two α-helices (α_2, α_3) and one β-strand (β_6). The major structural difference compared to the plant-type ferredoxins is the presence of a

more compact structure in the C-terminal half of the protein, which is mainly formed by the side-chains of residues His49, Tyr51, Val74, Ala76, Leu78 and the C-terminal peptide Pro102–Trp106. The side-chain of the functionally important Trp106 is highly solvent exposed in Pdx (Pochapsky et al., 1994a).

The dependence of the Pdx structure and dynamics on the redox state was assessed by measuring proton chemical shifts and amide proton exchange rates in the oxidized and reduced state, respectively (Pochapsky et al., 1994b; Lyons et al., 1996). The largest chemical shift changes observed upon changing the redox state that are not caused by hyperfine interactions were reported for the C-terminal residues and for the Val74–Ala76 loop (Pochapsky et al., 1994b). In the corresponding regions redox dependent differences in the protein dynamics were revealed by amide proton exchange studies. In general, amide protons exchange more rapidly in the oxidized form of the protein than in the reduced form, showing the largest differences for the residues in the cluster vicinity, residues Val74–Ser82 and the C-terminal residues, Pro102–Trp106 (Lyons et al., 1996). The observation that the oxidation state of the cluster strongly affects the protein dynamics suggests a possible mechanism for modulating binding of redox partners without large conformational changes (Lyons et al., 1996).

A model of the P-450$_{cam}$–Pdx complex, which is limited to the prediction of gross structural features, suggests a close distance of 12 Å between the metal centers of the two proteins and aromatic interactions between Trp106 of Pdx and Tyr78 and His352 of P-450$_{cam}$ (Pochapsky et al., 1996).

One approach to refine the NMR solution structure of iron–sulfur proteins is to replace the iron atoms of the cluster by diamagnetic metals, preventing paramagnetic line broadening and thus allowing assignment of resonances from residues in the cluster vicinity.

Reconstitution of Pdx using Ga^{3+} yielded a stable mononuclear rubredoxin-like (GaS_4) gallium derivative which was shown to retain the secondary structure and global fold of native Pdx. Structural differences are mainly limited to the flexible cluster binding loop, which appears sufficiently distortable to accommodate different metal binding geometries (Kazanis et al., 1995). Differences were also noted for the amide proton exchange rates that are considerably faster in the Ga-substituted Pdx than in the wild-type (Kazanis and Pochapsky, 1997).

Non-denaturating substitution of cluster irons by other metals was also studied on spinach ferredoxin and bovine adrenodoxin (Iametti et al., 1996). The Zn^{2+} and Cd^{2+} substituted proteins lost their electron transferring capability and showed loss of secondary structure compared to the wild-type protein. However, these altered structural features did not impede the reincorporation of iron, which resulted in the restoration of the native structure (Iametti et al., 1996).

2.6. Aldehyde oxido-reductase of Desulfovibrio gigas

The aldehyde oxido-reductase of *D. gigas* contains a molybdenum cofactor (Mo-co) and two [2Fe–2S] clusters that proved to be spectroscopically different (Barata et al., 1992). The crystal structure with a resolution of 2.25 Å (Romao et al., 1995) revealed that the first cluster binding domain has a structure similar to those found in plant-type [2Fe–2S] ferredoxins consisting of a five-stranded β-sheet and an α-helix. The two iron atoms of the cluster are linked to Cys40

and Cys45 and Cys48 and Cys60, respectively. Minor differences to plant-type ferredoxins include a shorter loop connecting strands β_1 and β_2 of the β-sheet and the lack of the loop corresponding to amino acids 54–73 (Romao et al., 1995).

The domain containing the second cluster shows a fold that has not been described previously for [2Fe–2S] proteins (Fig. 2d): the iron-sulfur cluster is located at the N-terminus of two α-helices, which are part of a twofold symmetric four-helix bundle and the cluster is buried in the interior of the protein approximately 15 Å below the protein surface. A new pattern for the cluster ligation is present in which the first iron of the cluster is linked to Cys100 and Cys139 and the second iron to Cys103 and Cys137. A similar spacing of cysteine residues has also been reported for the C-terminal cluster of the *CoxS* subunit of carbon monoxide dehydrogenase from *Oligotropha carboxidovorans* (Schübel et al., 1995).

Aldehyde oxido-reductase from *D. gigas* shows a sequence similarity (identity) of 52% (26%) to the xanthine oxidase of *Drosophila melanogaster* that is particularly high in regions associated with the iron–sulfur clusters and the molybdopterin (Thoenes et al., 1994; Huber et al., 1996). This finding suggests that the chain fold discovered for the second iron–sulfur cluster in *D. gigas* aldehyde oxido-reductase may be a widespread motif in this family of proteins.

3. Low-potential ferredoxins containing [4Fe–4S] or [3Fe–4S] clusters

Low-potential [4Fe–4S] ferredoxins show the redox states $[4Fe–4S]^{2+/+}$ and reduction potentials from −250 to −650 mV (Yoch and Carithers, 1979; Armstrong et al., 1988), in contrast to the high-potential iron–sulfur proteins (HiPIPs) which have positive potentials of +50 to +500 mV for their $[4Fe–4S]^{3+/2+}$ clusters. Low-potential [4Fe–4S] ferredoxins often obtain three of their four cluster ligands from a highly conserved CysXXCysXXCys sequence motif. The fourth cysteine is provided by a more remote part of the peptide chain. The family of low-potential ferredoxins does not only include ferredoxins with one or two [4Fe–4S] clusters but also molecules with a single [3Fe–4S] or one [3Fe–4S] and one [4Fe–4S] cluster, which are functionally similar.

Typically, redox potentials of approximately −400 mV are observed for electron-transferring [4Fe–4S] ferredoxins (Berg and Holm, 1982; Feinberg et al., 1997). However, the actual potentials range from −280 mV, reported for *Bacillus stearothermophilus* ferredoxin (Jensen et al., 1994), to the unusually low value of −645 mV measured for the [4Fe–4S] cluster of the [4Fe–4S][3Fe–4S] ferredoxin from *Azotobacter vinelandii* (Iismaa et al., 1991; Langen et al., 1992).

For [3Fe–4S] clusters, commonly redox potentials of −100 to −150 mV are reported (e.g. −130 mV for *D. gigas* ferredoxin II (Cammack et al., 1977b)). Several unusual features distinguish the [3Fe–4S] cluster in *Azotobacter vinelandii* ferredoxin (Fd_{Av}) from those found in other proteins: the formal reduction potential of this cluster (∼ −420 mV) at neutral pH is significantly lower than that of other [3Fe–4S] clusters and a strong pH dependence was observed for the redox potential of this cluster (Iismaa et al., 1991). Furthermore, unlike the [3Fe–4S] clusters of *D. gigas* ferredoxin II (Moura et al., 1982), *D. africanus* ferredoxin III (George et al., 1989), or *P. furiosus* ferredoxin (Busse et al., 1992), the [3Fe–4S] cluster of Fd_{Av}

cannot be converted to a [4Fe–4S] cluster by adding Fe^{2+} under reducing conditions (Morgan et al., 1984). However, a conversion has been achieved in the presence of the denaturating agent guanidine hydrochloride (Shen et al., 1993).

Cluster conversion was studied for *D. africanus* ferredoxin III, which possesses a [3Fe–4S] cluster and a [4Fe–4S] cluster with redox potentials of −140 mV and −410 mV, respectively (Armstrong et al., 1989). Addition of Fe^{2+} to the reduced [3Fe–4S] cluster resulted in a [4Fe–4S] cluster with a characteristic redox potential of −400 mV (George et al., 1989). A detailed summary of techniques used for studying redox potentials and of the redox potentials determined thus far is given elsewhere (Smith and Feinberg, 1990; Smith et al., 1991c; Jensen et al., 1994; Smith et al., 1995; Feinberg and Ryan, 1996).

Generally, low-potential ferredoxins function as electron carrier proteins and are found in all organisms which are consuming or producing hydrogen (for a review see Bruschi and Guerlesquin, 1988). Various organisms use these ferredoxins for different purposes, as low-potential electron carriers, particularly in anaerobic metabolism and they have probably more different functions than any other iron–sulfur protein (Cammack, 1992).

The monocluster ferredoxins from *P. furiosus* and *T. maritima* act as electron transfer proteins between pyruvate oxidoreductase and a terminal hydrogenase (Blamey and Adams, 1994). Ferredoxin I from *Rhodobacter capsulatus* probably participates in nitrogen fixation (Jouanneau et al., 1995a; Saeki et al., 1996) and *D. vulgaris* Miyazaki ferredoxin I was proposed to be the electron carrier in the phosphoroclastic reaction for pyruvate

Table 4
Structure-based sequence alignment of several bacterial [4Fe–4S] and [3Fe–4S][4Fe–4S] ferredoxins. Sequence alignment of the [3Fe–4S][4Fe–4S] ferredoxin from *Azotocacter vinelandii* (Howard et al., 1983) and of the 2[4Fe–4S] ferredoxins from *Chromatium vinosum* (Hase et al., 1977b), *Peptostreptococcus asaccharolyticus* (Backes et al., 1991), *Clostridium pasteurianum* (Tanaka et al., 1966) and *Clostridium acidurici* (Meyer et al., 1993)

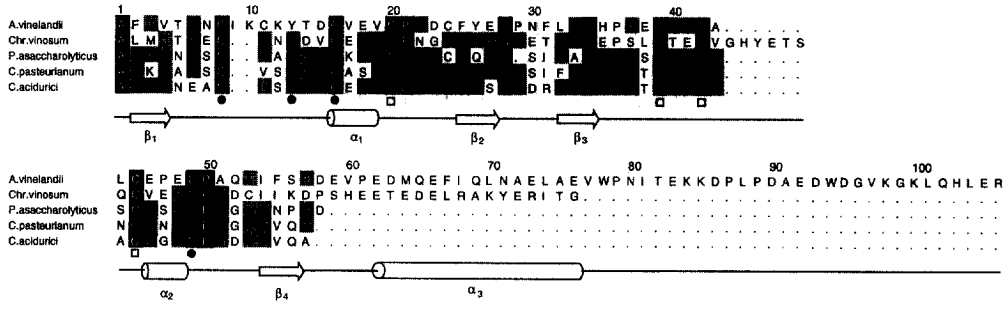

The *A. vinelandii* numbering scheme is given at the top. The sequence positions of the ligating cysteines of the first and second cluster are indicated by black circles (●) and rectangles (□), respectively. Strictly conserved residues at one position are highlighted by a black box and residues occurring with a frequency of ≥50% are marked by gray boxes. Elements of the secondary structure present in the *A. vinelandii* structure (Merritt et al., 1993) are given below the alignment.

The alignment was generated using the programs ClustalW (Higgins et al., 1992) and Alscript (Barton, 1993).

dehydrogenase coupled with hydrogenase and cytochrome c_3 (Ogata et al., 1988). The electron transfer function of *A. vinelandii* ferredoxin I was found to be important for cell growth (Martin et al., 1989; Iismaa et al., 1991) and the protein has a regulatory function in controlling the expression of the *fpr* gene product (Martin et al., 1989; Isas and Burgess, 1994; Isas et al., 1994). For the [7Fe–8S] ferredoxin from *Streptomyces griseus* a function as electron transport protein for the cytochrome-P450 system from the same organism has been reported (Trower et al., 1990).

3.1. Low-potential ferredoxins of the dicluster type

Crystal structures are available for the 2[4Fe–4S] ferredoxins from *Peptostreptococcus asaccharolyticus* (formerly *Peptococcus aerogenes*) (Fd_{Pa}, Adman et al., 1973, 1976; Backes et al., 1991), *Clostridium acidurici* (Fd_{Ca}, Duée et al., 1994; Tranqui and Jesoir, 1995), *Chromatium vinosum* (Fd_{Cv}; Moulis et al., 1996a) and for the [3Fe–4S][4Fe–4S] ferredoxin from *Azotobacter vinelandii* (Fd_{Av}; Stout, 1989; Merritt et al., 1993). In addition, the structure of *Clostridium pasteurianum* ferredoxin, a close relative of *Clostridium acidurici* ferredoxin, has been derived from NMR data (Fd_{Cp}; Bertini et al., 1995a).

The alignment in Table 4 shows high sequence similarities between the amino acid sequences of bacterial dicluster ferredoxins in their N-terminal ~60 amino acids. The ferredoxins differ mainly in the C-terminal sequence following the coordination motif of the second cluster. The

Table 5
Sequence comparison with thermoacidophilic archaeal ferredoxins. Sequence alignment of the thermoacidophilic archaeal ferredoxins from *Sulfolobus* sp. (Fujii et al., 1997) and *Thermoplasma acidophilum* (Wakabayashi et al., 1983) and three bacterial ferredoxins

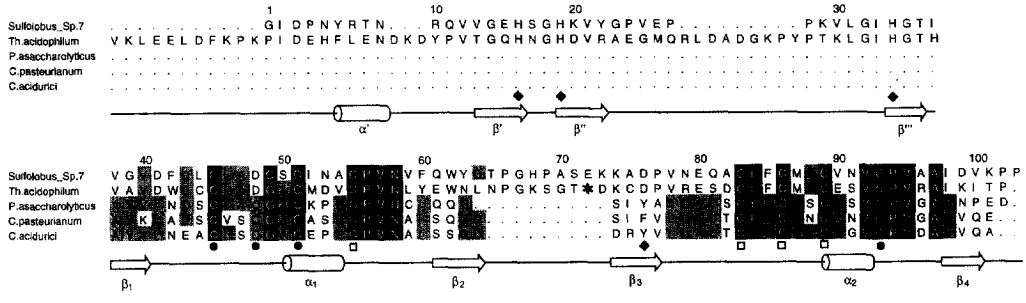

The *Sulfolobus* sp. numbering scheme is given at the top. The sequence positions of the ligating cysteines of the first and second cluster are indicated by black circles (●) and rectangles (□), respectively. Positions of those residues ligating the zinc ion in the thermoacidophilic ferredoxins are marked by black diamonds (◆). An asterisk indicates an insertion of 18 residues (GNDHKIQKGSEEWNKYRT) in the *T. acidophilum* sequence. Strictly conserved residues at one position are highlighted by a black box and residues occurring with a frequency of ≥50% are marked by gray boxes. Elements of secondary structure present in the *Sulfolobus* sp. structure (Fujii et al., 1996) are given below the alignment.
The alignment was generated using the programs ClustalW (Higgins et al., 1992) and Alscript (Barton, 1993).

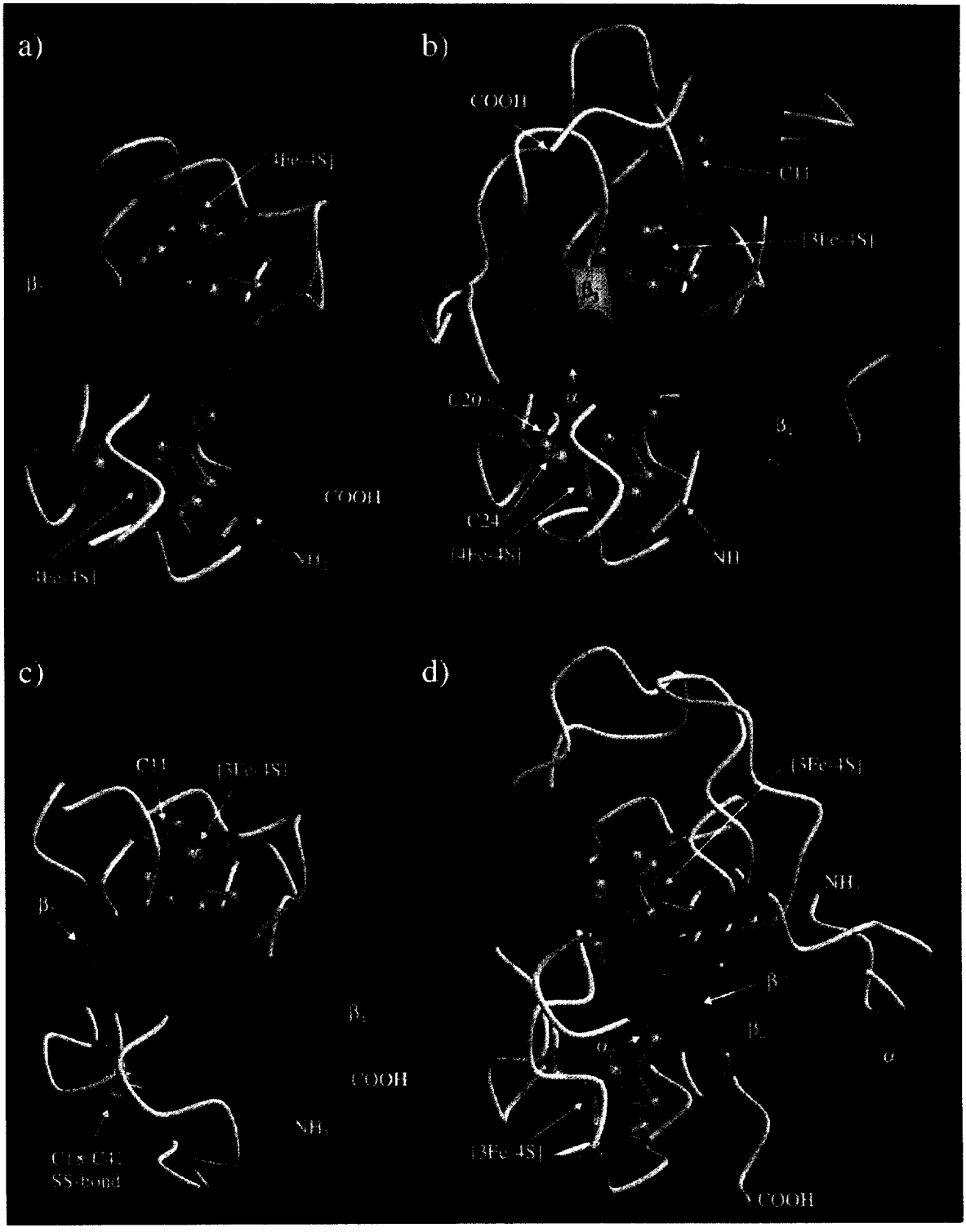

Fig. 3. *Caption opposite*

Clostridium-type ferredoxins stop a few amino acids after this motif, whereas the *Azotobacter*-type ferredoxins have longer C-terminal extensions (Moulis et al., 1996a). In the thermoacidophilic ferredoxin from *Sulfolobus* sp. (Fujii et al., 1996) a long N-terminal extension is present (Table 5).

After exclusion of these N- or C-terminal extensions, all molecules show roughly C_2-symmetry which is not only present for the iron-sulfur clusters but also for the main chain topology and most of the side chains (Fig. 3a).

The clusters have the shape of a distorted cube, with the Fe and S atoms at the alternate corners: these atoms form two interpenetrating tetrahedrals that show a strictly conserved geometry among all [4Fe–4S] ferredoxins. The average distances and angles reported for Fd_{Ca} are (Duée et al., 1994): Fe–S, 2.26 Å; S–S, 3.55 Å; Fe–Fe, 2.75 Å; Fe–S–Fe, 75°; S–Fe–S, 103°. The iron atoms of the cluster are attached to the polypeptide chain by four covalent Fe–Sγ bonds involving cysteines. A total of eight conserved main chain amide hydrogen bonds is found to the sulfur atoms of the cluster (Backes et al., 1991). The clusters are shielded from direct interactions with the solvent by a number of hydrophobic amino acid residues (Duée et al., 1994; Moulis et al., 1996a).

Fd_{Pa} (Adman et al., 1976; Backes et al., 1991), Fd_{Ca} (Duée et al., 1994) and Fd_{Cp} (Bertini et al., 1995a) each contain 55 amino acids and the very similar overall folding of the molecules is stabilized by a core of hydrophobic side chains, a network of hydrogen bonds involving main chain and side chain atoms and several water molecules. The N- and C-termini contribute strands β_1 and β_4 to the antiparallel β-sheet A and an additional β-sheet B formed by strand β_2 and β_3 of a loop region (Fig. 3a). The sequence regions connecting CysIII of one cluster with CysIV of the other cluster fold as distorted helical segments (α_1, α_2 in Fig. 3a) (Duée et al., 1994). Some of the water molecules play a structural role by stabilizing the N-terminal β-sheet A (Fd_{Ca}) or by bridging the two β-sheets A and B (Fd_{Ca}; Fd_{Cv}) thus forming a pseudo β-sheet (Duée et al., 1994; Moulis et al., 1996a).

Two additional unique features have been described for Fd_{Cv} (Moulis et al., 1996a): a six residue insertion between two ligands of one cluster which forms a two-turn external loop (Table 4). This loop causes conformational changes of one cysteine ligand and impedes the formation of one amide hydrogen bond to an inorganic sulfur. The second new structural

Fig. 3. Schematic ribbon representation of the three-dimensional structures of various low potential ferredoxins containing [4Fe–4S] or [3Fe–4S] clusters: Elements of regular secondary structure are indicated and labeled according to the nomenclature in Tables 4–6. The iron–sulfur clusters, their ligating cysteines and other important residues are shown in ball-and-stick presentation. All figures were generated using the programs MOLSCRIPT (Kraulis, 1991) and Raster3D (Bacon and Anderson, 1988; Merritt and Murphy, 1994). (a) Structure of the 2[4Fe–4S] dicluster ferredoxin from *Clostridium acidurici* (Duée et al., 1994). (b) Structure of the [3Fe–4S][4Fe–4S] dicluster ferredoxin from *Azotobacter vinelandii* (Merritt et al., 1993). In order to facilitate the comparison, the same orientation as in (a) is shown. The C-terminal extension, that is not present in the *Clostridium*-type ferredoxins is starting from helix α_3. In addition to the cluster-ligating cysteines, the free cysteines Cys11 and Cys24 are shown in ball-and-stick representation. (c) Structure of the [3Fe–4S] monocluster ferredoxin from *D. gigas* (Kissinger et al., 1991). In order to facilitate the comparison, the same orientation as in (a) is shown. The free Cys11 occupies the sequence position of the fourth cluster ligand in the [4Fe–4S] ferredoxins and a disulfide bond is present between Cys18 and Cys41. (d) Structure of the thermoacidophilic ferredoxin from *Sulfolobus* sp. (Fujii et al., 1996). In order to facilitate the comparison, the same orientation as in (a) is shown. The N-terminal extension, that is not present in bacterial dicluster ferredoxins includes helix α' and β-strands β', β'' and β'''.

element is a 3.5-turn α-helix at the C-terminus that covers one side of the cluster and is linked to the cluster binding domain by a short segment of six residues. These structural features are the likely cause (Moulis et al., 1996a) of the very low reduction potential around −500 mV (Smith and Feinberg, 1990) and of the significantly slower rate of intramolecular electron transfer between the clusters compared to Fd_{Ca} and Fd_{Cp} (Huber et al., 1995).

In contrast to the ferredoxins described above, Fd_{Av} contains one [3Fe–4S] and one [4Fe–4S] cluster (Fig. 3b). The geometry of the [3Fe–4S] cluster is a regular, cubane-like structure, with an iron atom corresponding to one corner missing. The geometry of the cluster and the hydrogen bonding pattern is virtually identical to the known [4Fe–4S] structures (Stout, 1989).

Interestingly, superposition of the main chain topologies of Fd_{Av} with 106 residues and of Fd_{Pa} with 55 residues showed a striking similarity within residues 1–58 of the former, after exclusion of residues 9, 10 and 28–31 (Merritt et al., 1993). The latter residues are part of two loops which are in contact with the residues of the extended C-terminal chain of Fd_{Av} (Fig. 3b). Fd_{Av} contains similar elements of secondary structure in the same positions as the 2[4Fe–4S] ferredoxins (Fig. 3a and b). The C-terminal extension after Asp58 bends into a three-turn helix from residue 64 to 75 followed by loops that wrap around one side of the body of the molecule (Merritt et al., 1993).

A comparison of the C-terminal extension to that present in Fd_{Cv} revealed that length, structure and orientation are different in these proteins suggesting a divergent evolution within the family of the dicluster ferredoxins. The latter additions may have occurred independently as evidenced by the lack of sequence homology and by the completely different fold of Fd_{Av} and Fd_{Cv} (Moulis, 1996; Moulis et al., 1996a).

Additional information about the evolution of ferredoxins can be obtained from the position of the free cysteines in Fd_{Av}. There are two free cysteine sulfhydryl groups in Fd_{Av} (Cys11, Cys24) and each of them is adjacent to one of the iron–sulfur clusters (Fig. 3b). Cys24 is located in close proximity to one inorganic sulfur of the [4Fe–4S] cluster of Fd_{Av} and Cys11 is part of a reverse turn $C^{8}IKC^{11}$, where Cys8 is a ligand of the [3Fe–4S] cluster. During the evolution of the seven-iron ferredoxins from the eight-iron ferredoxins two residues were inserted in the CysXXCysXXCys sequence motif between the second and third cysteine to form a CysXXCysXXXXCys motif (Bruschi and Guerlesquin, 1988). The insertion of residues 9 and 10 compared to Fd_{Pa} moved the second cysteine away from the cluster resulting in the inability to form a $[4Fe–4S]^{2+/+}$ cluster and the appearance of a $[3Fe–4S]^{+/0}$ cluster in that position (Adman et al., 1973, 1976; Stout, 1989; Backes et al., 1991).

Fd_{Av} has been the subject of numerous mutational studies, which were discussed on the basis of the three-dimensional structure available for the mutants. Some of the mutations were addressed to study the ligand binding properties of the cluster. Exchange of Cys20, a ligand of the [4Fe–4S] cluster, for alanine causes Cys24, a free residue in the native protein, to become a cluster ligand (Martin et al., 1990). Even when Cys20 is changed to serine, the cluster rejects oxygen ligation in favour of sulfur ligation to Cys24 (Shen et al., 1995). The structures of both mutants are remarkably similar, but show considerable differences to the wild-type protein, as a consequence of an 'iron–sulfur cluster driven protein rearrangement' (Shen et al., 1995). On exchange of Cys24 to alanine the structure remained similar to native Fd_{Av}, but higher B-factors indicated the loss of tight packing (Iismaa et al., 1991, Soman et al., 1991). While the redox potentials of the [4Fe–4S] cluster of the mutants (C20A, −746 mV; C24A, −600 mV)

differ significantly from the value reported for the native protein (–647 mV), no changes were observed for the [3Fe–4S] cluster (Iismaa et al., 1991).

Exchange of Tyr13 of Fd_{Av} for cysteine, which occupies the position of the fourth ligating cysteine in the structurally homologous 2[4Fe–4S] ferredoxins, was intended to direct the conversion of the [3Fe–4S] cluster to a [4Fe–4S] cluster (Kemper et al., 1997). The three-dimensional structure revealed, however, that the protein mutant fails to use Cys13 as a ligand and retained its [3Fe–4S] cluster. Interestingly, the introduced cysteine was modified to become a persulfide, possibly due to the activity of *Nif*S or a *Nif*S-type enzyme (Zheng and Dean, 1994), which might specifically recognize and modify this residue on the basis of a yet unknown structural motif (Kemper et al., 1997). Although the structure is extremely similar to the native Fd_{Av}, the mutant shows significantly decreased stability in the reduced state, which was attributed to loss of hydrophobic contacts, exposure of additional hydrophobic surface area or decreased shielding of the cluster by the smaller side chain of Cys13 (Kemper et al., 1997). Interestingly, a different behavior is observed for the D13C variant of *Bacillus schlegelii* 7Fe ferredoxin. In this protein Cys13 is able to serve as a ligand to the new fourth iron atom of the cluster despite the presence of an atypical cluster binding sequence (CysXXXXCysXXCys) (Aono et al., 1997).

Another series of Fd_{Av} mutants was intended to investigate the structural basis of the pH dependence of the redox potential and the role of the peptide chain in modulating the redox properties of the [3Fe–4S] cluster.

Structure determination of Fd_{Av} at pH 8 and 6 for both the oxidized and reduced state (Stout, 1993) had shown that the major structural change that occurs upon reduction at high pH is the movement of the negatively charged Asp15 away from the [3Fe–4S] cluster, while reduction at low pH or the change of pH from 8 to 6 did not have any significant effect on the [3Fe–4S] cluster or Asp15. Mutation of Asp15 to asparagine resulted in loss of the Asp15–Lys84 salt bridge, but the structure of the [3Fe–4S] cluster was conserved (Shen et al., 1993). The observation that the pH dependence of the redox potential is preserved in the mutant led to the conclusion that it originates from a direct protonation of the [3Fe–4S] cluster, probably on a sulfide ion (Shen et al., 1993). It was proposed that Asp15 of the native protein facilitates the proton transfer in its ionized state, thus explaining the overall slower protonation and deprotonation for the asparagine mutant (Shen et al., 1993).

Reasons for the differences in the redox potentials of the [4Fe–4S] clusters observed between Fd_{Av} and Fd_{Pa} (which has a less negative E^0) were investigated by six Fd_{Av} mutants in which individual residues were converted into those residues found in Fd_{Pa} at the corresponding sequence positions (Shen et al., 1994). Four of the mutations substituted negatively charged surface residues with neutral residues and two mutations substituted buried hydrophobic residues. With exception of the F25I mutant, which showed significant structural changes and minor changes in E^0, there were no changes in the reduction potential for the other mutants, showing that surface residues do not account for the differences in the reduction potential between the [4Fe–4S] clusters of Fd_{Av} and Fd_{Pa} (Shen et al., 1994).

Mutational studies were also carried out for the ferredoxins from *Clostridium pasteurianum* (Smith et al., 1991b; Gaillard et al., 1993; Quinkal et al., 1994, 1996; Moulis and Davasse, 1995; Feinberg et al., 1997; Kyritsis et al., 1997) and *Rhodobacter capsulatus* (Naud et al., 1996; Saeki et al., 1996) probing thermal stability, redox properties and structural aspects influencing

the inter- and intramolecular electron transfer. Three-dimensional structures for these mutants, however, are not available up to now.

In contrast to native Fd_{Cp}, which shows a pH-independent redox potential of −413 mV, the redox potential of a Y2H mutant was −343 mV and −394 mV at pH 6.4 and 8.7, respectively. The observed pH-dependent reduction potential for a Fd_{Cp} that contains His2 was attributed to the electrostatic interactions between His2 and iron sulfur cluster II which is approximately 6 Å away (Smith et al., 1991a,b). Although His2 is commonly found in thermostable clostridial ferredoxins, the Y2H substitution in Fd_{Cp} did not significantly increase its thermostability.

Additional mutational studies focused on the two highly conserved residues Pro19 and Pro48, which have been substituted by different amino acids (Gaillard et al., 1993). In all variants the protein fold and the electronic structure of the cluster were unaltered as evidenced by NMR and EPR spectroscopy. With the exception of the P19K mutation, the biological activity was similar to that reported for the native protein and the reduction potentials of all variants fell within a narrow range of less than 20 mV above the potential of the native protein. In general, however, destabilization of the structure, as evidenced by an increased rate of denaturation was observed for either mutant, indicating that the conserved prolines stabilize the active site but do not play an essential role in the mechanism of electron transfer (Quinkal et al., 1994). Similar results were obtained from site-directed mutagenesis of the two aromatic residues Tyr2 and Tyr30, implying that the electron transfer from the clusters is not mediated by those residues. Rather, these residues appear to be involved in maintaining a stable overall fold of Fd_{Cp} (Quinkal et al., 1996).

An extensive mutational study in which all conserved glutamates and aspartates were converted into neutral or positively charged amino acids was initiated to investigate the role of electrostatic forces for the interaction of Fd_{Cp} with its redox partners, pyruvate–ferredoxin oxidoreductase and hydrogenase (Moulis and Davasse, 1995). Electrostatic forces proved to be not crucial for these interactions as they are almost independent of number and distribution of anionic side chains on the ferredoxin surface (Moulis and Davasse, 1995). Recent studies, which determined the intramolecular electron transfer rate between the two clusters in Fd_{Cp} and a number of mutants, did not reveal any specific amino acid side chain that plays a central role in this process (Kyritsis et al., 1997).

Chemical synthesis of entire ferredoxins, which was applied previously for the synthesis of the *C. pasteurianum* Y2H mutant (Smith et al., 1991a), provided the basis for studies using non-naturally occurring amino acids (Feinberg et al., 1997). Cys11, a ligand of the [4Fe–4S] cluster in Fd_{Cp}, was substituted by glycine, aspartate and α-aminobutyric acid (Aba). For the Asp and Aba mutant, both clusters remained intact, however, the reconstitution of the C11G mutant failed due to its low stability. Both the Asp and the Aba mutant were less stable than the native protein upon exposure to oxygen, suggesting that mutation of any of the cluster ligands resulted in considerably more unstable proteins (Feinberg et al., 1997).

One major aspect of mutational studies of *Rhodobacter capsulatus* ferredoxin I (Fd_{Rc}) was the identification of amino acids possibly involved in the interaction with dinitrogenase reductase (Naud et al., 1996; Saeki et al., 1996). These studies revealed the importance of the acidic residue Asp36 for binding to dinitrogenase reductase, while a double mutant in which Lys27 and Lys28 were substituted with glutamate, indicates that these basic residues have no critical role in that process (Naud et al., 1996). Replacement of amino acids 42–49 by a Gly–

Ala sequence shows that the corresponding residues do not contribute to nitrogen fixation, but may be involved in modulation of the redox potential of one of the two clusters (Saeki et al., 1996). Additional results from site-directed mutagenesis studies on the coordination sphere of iron–sulfur clusters are summarized in a recent review by Moulis et al. (1996b). Numerous NMR and EPR investigations of the electronic and magnetic structure of iron–sulfur proteins are dealt with in detail elsewhere (Beinert, 1990; Bertini et al., 1993, 1995b, 1996c; Cheng and Markley, 1995; Beinert et al., 1997).

One particular aim of recent NMR studies was to obtain structural information about iron sulfur proteins, for which no sequence or structural data is available. The 1D-NMR data collected for a variety of ferredoxins showed a correlation between the protein sequence and the chemical shifts of the β-methylene protons of the cysteines that ligate the cluster (Bertini et al., 1997a). Analysis of the pattern of hyperfine shifts furthermore allows comparison of the degree of homology to known three-dimensional structures and provides the basis for model-building.

This approach has been applied to the ferredoxins from *Clostridium pasteurianum* (Busse et al., 1991; Bertini et al., 1994b), *Bacillus schlegelii* (Aono et al., 1996), *Rhodopseudomonas palustris* (Bertini et al., 1997a), *Desulfovibrio africanus* (Davy et al., 1995) and *Desulfurolobus ambivalens* (Bentrop et al., 1996b), as well as to the PsaC protein of the photosystem I complex (Bentrop et al., 1997). These studies thus may offer a promising approach for solution studies of larger iron sulfur proteins such as hydrogenases, dehydrogenases or aconitases (Bertini et al., 1997a).

3.1.1. The F_A/F_B protein (PsaC) of the photosystem I complex

The photosystem I (PS I) contains three clusters of the [4Fe–4S] type, denoted as X, A and B. The F_A/F_B protein encoded by the *psaC* gene is a small protein of approximately 8–9 kDa, which carries the centers A and B. Amino acid sequences of several F_A/F_B proteins are known, for example from chloroplasts of spinach (Oh-oka et al., 1988), tobacco (Hayashida et al., 1987), liverwort (Ohyama et al., 1986), maize (Schantz and Bogorad, 1988), barley (Hoj et al., 1987), pea and wheat (Dunn and Gray, 1988) and from the cyanobacterium *Synechococcus vulcanus* (Koike et al., 1989).

The sequences are highly conserved and share approximately 80% sequence homology among the proteins from different organisms (Oh-oka et al., 1988). Apart from the presence of two characteristic [4Fe–4S] cluster binding motifs, there is only a moderate sequence homology to the bacterial dicluster ferredoxins (Hayashida et al., 1987; Hoj et al., 1987).

The crystal structure of PS I from the thermophilic cyanobacterium *Synechococcus elongatus*, which was recently determined at a 4 Å resolution (Krauß et al., 1996), gives new insight into the location and the structure of the PsaC subunit.

PsaC is located on the stromal side of the transmembrane subunits PsaA and PsaB of PS I. PsaC occupies the central position of the stromal ridge of PS I and is flanked by two additional stromal subunits PsaD and PsaE (Krauß et al., 1996). All three stromal subunits have been reported to play a role as docking site for ferredoxin or flavodoxin, which act as electron acceptors for PS I upon reduction (Rousseau and Lagoutte, 1993; Chitnis et al., 1995; Lelong et al., 1996).

The structure at 4 Å resolution allowed the identification of the position of the two [4Fe–4S] clusters and of two short helical segments (Krauß et al., 1996). Similar to the bacterial dicluster ferredoxins, a two-fold symmetry axis is present in PsaC, which relates the two iron sulfur clusters that are 12 Å apart.

PsaC was proposed on the basis of the electron densities to have a three-dimensional structure very similar to 2[4Fe–4S] Fd_{Pa}. Larger differences are only observed for the N- and C-termini of PsaC and for a central loop that is not present in Fd_{Pa} (Krauß et al., 1996). This similarity to bacterial dicluster ferredoxins was recently confirmed by NMR spectroscopic studies of the unbound PsaC subunit (Bentrop et al., 1997).

The current resolution of the crystal structure does not allow an unambiguous assignment of the two clusters to F_A and F_B. Two possible orientations of PsaC in which either F_A or F_B is the proximal cluster to F_X are currently investigated by EPR studies (Kamlowski et al., 1997). On the assumption that the extended C-terminus points away from the membrane for steric reasons, it was suggested that F_B is the proximal and F_A the distal cluster, showing distances of 15 and 22 Å to F_X, respectively (Krauß et al., 1996).

3.1.2. Zinc-containing thermoacidophilic archaeal ferredoxins

A new class of ferredoxins has been identified exclusively in thermoacidophilic archaea such as *Sulfolobus acidocaldarius* (Minami et al., 1985; Breton et al., 1995), *Desulfurolobus ambivalens* (Teixeira et al., 1995) and *Thermoplasma acidophilum* (Wakabayashi et al., 1983). The ferredoxin from *Sulfolobus* sp. functions as an electron acceptor for the 2-oxoacid:Fd oxidoreductase (Kerscher et al., 1982; Iwasaki et al., 1994, 1995).

In contrast to the bacterial dicluster ferredoxins, *Sulfolobus* ferredoxin has an N-terminal extension of approximately 40 residues and an insertion of approximately 10 residues in the center of the peptide chain (Table 5 and Fig. 3d). Recently, the three-dimensional structure of *Sulfolobus* sp. strain 7 ferredoxin became available representing the first structure for this type of ferredoxins (Fujii et al., 1996).

The conformation of the molecule can be divided into a core fold (residues 37–103) and an N-terminal extension (residues 1–36). The crystal structure shows that the core fold which binds two [3Fe–4S] clusters is remarkably similar to the fold of bacterial dicluster ferredoxins (Fig. 3a).

EPR analysis and quantitative metal analysis of *Sulfolobus* sp. Fd and *T. acidophilum* Fd (Fujii et al., 1997; Iwasaki et al., 1997) and NMR spectroscopic studies of *D. ambivalens* Fd (Bentrop et al., 1996b) showed that these ferredoxins originally contain one [3Fe–4S] and one [4Fe–4S] cluster. The conformational heterogeneity detected in the NMR study of *D. ambivalens* (Bentrop et al., 1996b) and the peptide conformation in the crystal around the second cluster of *Sulfolobus* sp. Fd, which is intermediate between the [3Fe–4S] and [4Fe–4S] cluster conformations (Fujii et al., 1997), suggest that the [4Fe–4S] cluster is unusually unstable.

For the [3Fe–4S] cluster an incomplete cluster binding sequence is present, in which an aspartate (Asp48) occupies the position of the fourth cluster ligand. The midpoint redox potentials of the [3Fe–4S] and the [4Fe–4S] cluster of *Sulfolobus* Fd are −280 and −530 mV, respectively (Iwasaki et al., 1994).

The major structural differences between the core fold of *Sulfolobus* Fd and bacterial ferredoxins is an inserted loop (residues 65–72) which is located between strands β_2 and β_3 (Fujii et al., 1997). This structural element interacts with a loop present between the second and third strand of the β-sheet of the N-terminal extension (Fig. 3d).

The N-terminal extension (residues 1–36) consists of one turn of α-helix (α′) followed by a triple-stranded antiparallel β-sheet (β′, β″, β‴) (Fujii et al., 1996) which is hydrogen-bonded to β-sheet A of the core fold forming a larger, five-stranded β-sheet (β′, β″, β‴, β_1, β_4). A zinc binding motif is present at the interface between core fold and N-terminal extension, containing one zinc ion tetrahedrally coordinated by three histidines from the N-terminal part and one aspartate from the core fold (Fig. 4a). This motif was suggested to play an important role in stabilizing the structure by connecting the N-terminal extension and the core fold (Fujii et al., 1996, 1997).

Compared to *Sulfolobus* sp. ferredoxin, the N-terminal extensions of *S. acidocaldarius*, *D. ambivalens* and *T. acidophilum* Fd show sequence identities of 86, 86 and 57%, respectively (Fujii et al., 1997). A quantitative metal analysis has confirmed the presence of a zinc ion in addition to one [3Fe–4S] and one [4Fe–4S] cluster in *T. acidophilum* ferredoxin (Iwasaki et al., 1997), suggesting that a zinc binding ability might be a common feature of all thermoacidophilic archaeal ferredoxins.

Interestingly, an N-terminal extension which was proposed to play a role for protein stabilization has also been reported for the [2Fe–2S] ferredoxin from the halophilic archaeon *Haloarcula marismortui* (Frolow et al., 1996), however, this Fd does not contain a zinc binding site.

Several principles for the enhanced stability of thermoacidophilic archaeal ferredoxins have been deduced from the structure of *Sulfolobus* Fd, including the novel zinc ligation, the formation of a larger β-sheet, additional interactions of the inserted loop and indirect interactions between the two β-sheets mediated by the N-terminal extension (Fujii et al., 1997). Superposition of the structures revealed that the helix of the C-terminal extension of *Azotobacter vinelandii* Fd I coincides approximately with the N-terminal extension of *Sulfolobus* Fd (Fig. 3b and d). Based on this observation, indirect interactions between the two β-sheets, which are mediated by residues of the C-terminal extension in *Azotobacter vinelandii* Fd I (Stout, 1989) or by a pseudo β-sheet formed by water molecules in *Clostridium acidurici* ferredoxin (Duée et al., 1994) were proposed to generally stabilize the core fold of ferredoxins (Fujii et al., 1997).

3.2. Low potential ferredoxins of the monocluster type

Several bacteria produce ferredoxins with only a single [4Fe–4S] or [3Fe–4S] cluster. These clusters are interconvertible under certain conditions (Moura et al., 1982) and the biological significance of the presence of a [3Fe–4S] cluster is still under discussion (Bruschi and Guerlesquin, 1988; Kissinger et al., 1991).

The [4Fe–4S] ferredoxins are generally considered as having evolved from the 2[4Fe–4S] type by loss of two or more of the cysteines that bind the second cluster (Fukuyama et al., 1988). The iron–sulfur clusters are generally similar in function, redox potential and UV-spectral properties compared to the 2[4Fe–4S] type (Bruschi and Guerlesquin, 1988).

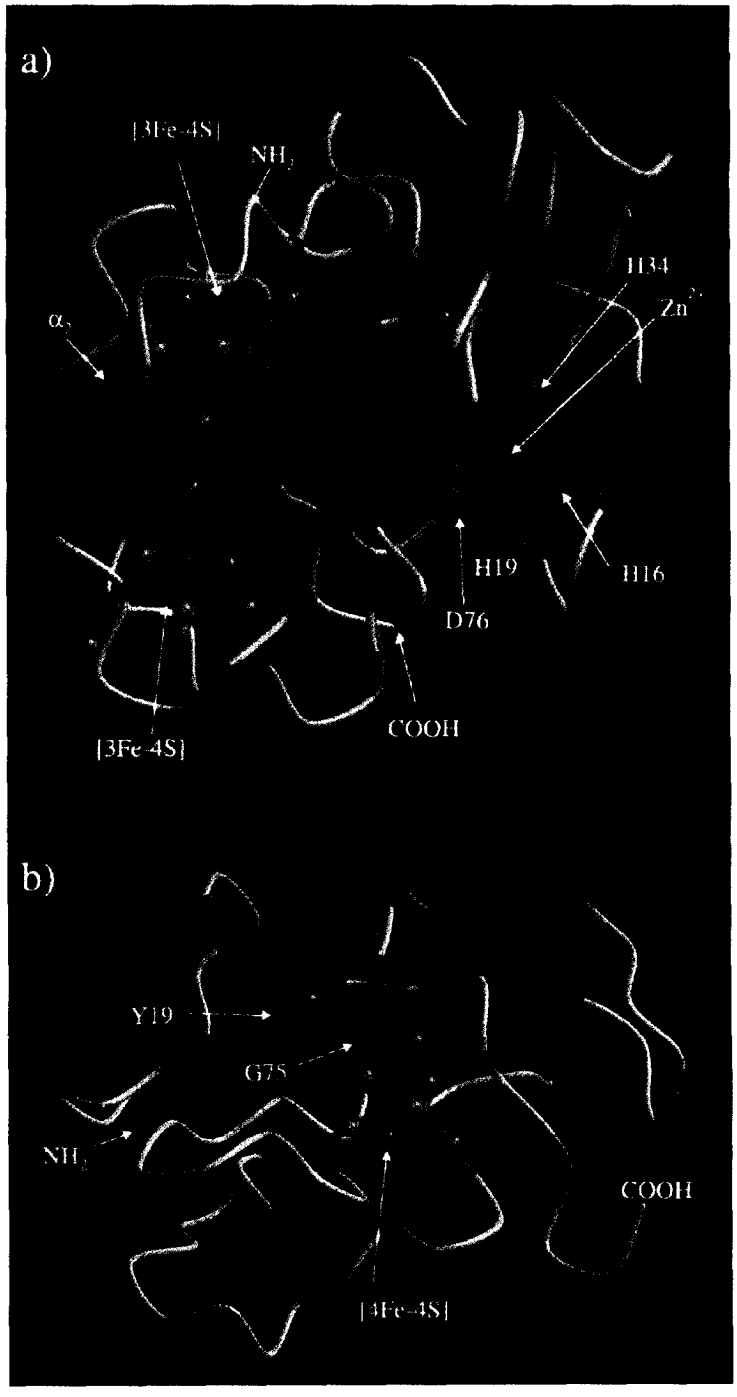

Fig. 4. Schematic ribbon representation of the three-dimensional structures of Sulfolobus sp. ferredoxin and *Chromatium vinosum* HiPIP: Elements of regular secondary structure are indicated and labeled according to the nomenclature in Tables 5 and 7. The iron–sulfur clusters, their ligating cysteines and other important residues are shown in ball-and-stick presentation. All figures were generated using the programs MOLSCRIPT (Kraulis, 1991)

Table 6
Structure-based sequence alignment of bacterial monocluster [4Fe–4S] and [3Fe–4S] ferredoxins from *Thermotoga maritima* (Darimont and Sterner, 1994), *Thermococcus litoralis* (Busse et al., 1992), *Pyrococcus furiosus* (Busse et al., 1992), *Bacillus thermoproteolyticus* (Fukuyama et al., 1988), *Desulfovibrio gigas* (Kissinger et al., 1991) and *Desulfovibrio africanus* (Séry et al., 1994)

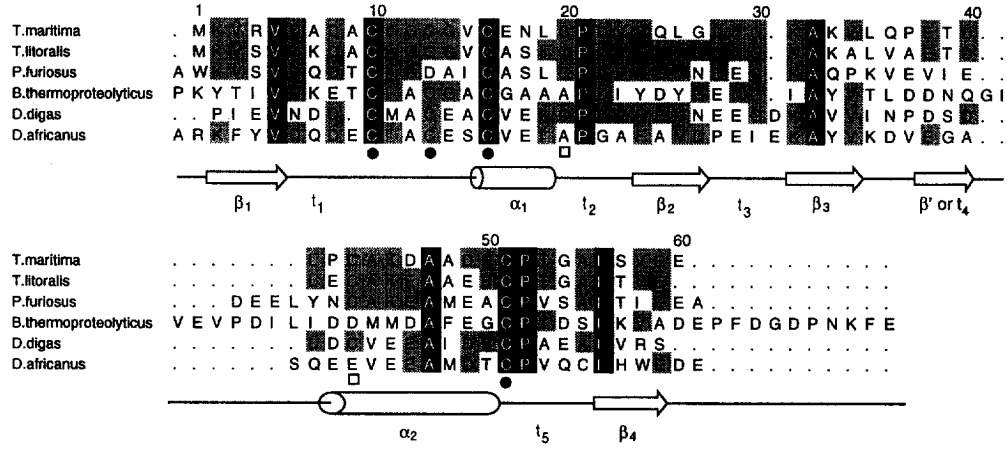

The *T. maritima* numbering scheme is given at the top. The sequence positions of the cluster ligating cysteines are marked by black circles (•). Rectangles (□) indicate the position of the cysteines involved in the disulfide bridge in *T. maritima*, *T. litoralis*, *P. furiosus*, and *D. gigas*. Strictly conserved residues at one position are highlighted by a black box and residues occurring with a frequency of ≥50% are marked by gray boxes. Common elements of secondary structure are given below the alignment.
The alignment was generated using the programs ClustalW (Higgins et al., 1992) and Alscript (Barton, 1993).

A sequence alignment of those monocluster-type ferredoxins, for which a three-dimensional structure is available, is shown in Table 6. For *Thermotoga maritima* Fd and for the archaeal Fd from *Thermococcus litoralis* (Fd_{Tl}), the solution structure has been calculated from NMR data (Donaire et al., 1994, 1996; Wildegger et al., 1995; Sticht et al., 1996; Wang et al., 1996) and for the ferredoxin from the archaeon *Pyrococcus furiosus* the secondary structure is known from NMR spectroscopy (Fd_{Pf}; Teng et al., 1994; Gorst et al., 1995a). Crystal structures have been determined for ferredoxin II from *Desulfovibrio gigas* (Fd_{Dg}; Kissinger et al., 1991), ferredoxin I from *Desulfovibrio africanus* (Fd_{Da}; Séry et al., 1994) and for the ferredoxins from

and Raster3D (Bacon and Anderson, 1988; Merritt and Murphy, 1994). (a) Detailed view of the structure of the thermoacidophilic ferredoxin from *Sulfolobus* sp. (Fujii et al., 1996). showing the relative location of the two iron–sulfur clusters and the zinc-binding motif in the protein. The N-terminal extension, that is not present in bacterial dicluster ferredoxins includes helix α′ and β-strands β′, β″ and β‴. Elements of secondary structure are labeled according to Table 5. (b) Schematic ribbon representation of the three-dimensional structure of the high-potential iron protein from *Chromatium vinosum* (Banci et al., 1995a). Tyr19 and Gly75, which are the only residues totally conserved among all HiPIPs, are shown in ball-and-stick representation.

Bacillus thermoproteolyticus (Fd_{Bt}; Fukuyama et al., 1988, 1989) and *Thermotoga maritima* (Fd_{Tm}; Macedo-Ribeiro et al., 1996).

With the exception of Fd_{Bt}, which has some insertions and a long C-terminal extension, all other ferredoxins consist of approximately 60 amino acids (Table 6). As already predicted from the high sequence similarity, all structures share a similar folding pattern and the pairwise backbone rmsd values are in the range of 1.5–2.0 Å.

The iron–sulfur cluster is covalently attached to the protein at residues 10, 13, 16 and 51 (according to the Fd_{Tm} numbering scheme) and has essentially the same geometry as the [4Fe–4S] clusters of the dicluster ferredoxins (Fig. 3c). The number and distribution of amide hydrogen bonds to the cluster as deduced from the crystal structures is conserved among Fd_{Tm}, Fd_{Da} and Fd_{Dg}.

In the [3Fe–4S] Fd II from *D. gigas*, the second cysteine in the sequence is not chelated with the cluster but is rotated and shows a solvent exposed side chain (Fig. 3c). The side chain could rotate to become the fourth cysteine ligand in a four iron form of the molecule, given a local readjustment of the peptide chain (Kissinger et al., 1991).

In Fd_{Pf}, an aspartate is found at the corresponding sequence position and was shown to be the fourth ligand of the cluster in each redox state (Calzolai et al., 1995). Whether Asp14 is a monodentate or a bidentate ligand of the cluster is still under investigation, but the observed differences in NMR hyperfine shifts between oxidized and reduced clusters suggest that this residue adopts different orientations with different cluster oxidation states. Different orientation or different ligation states were predicted to play a role in gating the electron transfer rate to the cluster (Calzolai et al., 1995, 1996). Site-directed mutagenesis of Asp14 to cysteine and serine has recently been applied to investigate the oxidation states of an individual iron atom in the cluster (Calzolai et al., 1997).

A disulfide bond is formed between two non-cluster-ligating cysteines in Fd_{Tl}, Fd_{Tm}, Fd_{Pf} and Fd_{Dg} (Table 6) and was shown to be involved in the redox cycle of Fd_{Dg} and Fd_{Pf} (Macedo et al., 1994; Gorst et al., 1995b). The disulfide bond, however, is not generally necessary for the stable folding of the single cluster ferredoxins (Kissinger et al., 1991) as evidenced by Fd_{Da} and Fd_{Bt}, which contain no cysteines at the corresponding sequence positions. Instead, these ferredoxins contain an alanine and a charged amino acid, respectively (Table 6).

All known monocluster ferredoxins possess two α-helices (α_1, α_2), two antiparallel β-sheets and four turns (t_1, t_2, t_3, t_5). The largest difference of the elements of secondary structure is that turn 4, which makes backbone contacts to the terminal β-sheet in all bacterial ferredoxins, is replaced by an extended sequence which forms a third antiparallel strand (β′) in the terminal β-sheet in Fd_{Tl} and Fd_{Pf}.

Tertiary side chain contacts are very similar among all ferredoxins. Aromatic residues are not essential for electron transfer, but combine with other hydrophobic amino acids to form a hydrophobic core that plays a crucial role for the stabilization of the iron–sulfur cluster (Fukuyama et al., 1988, 1989).

The folding topology of all monocluster ferredoxins in the cluster vicinity is similar to the folding topology of dicluster ferredoxins. An evolutionary model proposes that the monocluster type ferredoxins have evolved from the dicluster type by deletion of the second cluster and the emergence of a longer α-helix (α_2) in order to maintain a stable tertiary fold.

Divergent evolution of Fd_{Bt} and the other monocluster ferredoxins is the likely cause for the presence of the additional loop and the C-terminal extension in Fd_{Bt} (Fukuyama et al., 1988, 1989). The twofold symmetry axis observed in the dicluster ferredoxins has been lost in the monocluster ferredoxins during evolution (Fig. 3a and c).

An alternative evolutionary hypothesis was proposed recently on the basis of the observation that all known ferredoxins from early representatives of different phylogenetic domains contain a single [4Fe–4S] cluster. According to this hypothesis, dicluster ferredoxins have evolved from the monocluster type by the development of a second cluster binding site (Darimont and Sterner, 1994).

3.2.1. The structural basis for ferredoxin thermostability

In addition to the ferredoxin structures from two mesophilic (Fd_{Dg}, Fd_{Da}) and one moderately thermophilic organism (Fd_{Bt}), three ferredoxin structures from hyperthermophilic organisms are available (optimal growth temperature in parenthesis): *P. furiosus* (100°C), *T. litoralis* (90°C) and *T. maritima* (80°C). In contrast to *P. furiosus* and *T. litoralis*, both of which can be classified as archaea, *T. maritima* is one of the few representatives of hyperthermophilic bacteria. For the ferredoxin from *T. maritima* a denaturation temperature of 125°C was measured, one of the highest ever reported for a protein (Pfeil et al., 1997).

Before these structures became available, first conclusions on hyperthermostability were drawn from a number of functionally unrelated proteins from various organisms, revealing that proteins from hyperthermophiles do not possess structural motifs that differ significantly from those found in their mesophilic counterparts. Furthermore, no new type of structural interaction has been observed in these proteins. Instead, it appeared that a significantly enhanced thermostability is achieved by minor changes in secondary and tertiary contacts, including additional hydrogen bonds and salt bridges, increased volume to surface ratios and a higher content of elements of regular secondary structure (Jaenicke, 1991; Rees and Adams, 1995; Wang et al., 1996; Macedo-Ribeiro et al., 1997).

The knowledge of three ferredoxin structures from hyperthermophilic organisms allowed further investigations of the principles of thermostability, which are facilitated by the small size and the structural and functional similarity of these proteins.

A third strand (β′) of the terminal β-sheet (Fd_{Tl}, Fd_{Pf}), extension of helix α_2 (Fd_{Pf}), incorporation of the termini into a β-sheet structure (Fd_{Tl}, Fd_{Pf}, Fd_{Tm}) and better packing between the terminal β-sheet and helix α_2 (Fd_{Tl}, Fd_{Pf}) have been suggested as likely causes of thermostability (Teng et al., 1994; Wang et al., 1996; Macedo-Ribeiro et al., 1996, 1997).

In addition, residues in strained conformations are exchanged with glycines (Fd_{Tm}), the alanine content of α-helices is increased (Fd_{Tm}) and turn 3 which is located in the most flexible region of the protein is shorter in the thermophilic ferredoxins (Fd_{Tl}, Fd_{Pf}, Fd_{Tm}, Fd_{Bt}) than it is in their mesophilic counterparts (Sticht et al., 1996; Macedo-Ribeiro et al., 1996, 1997). Generally, the structure of Fd_{Tm} reveals an extended hydrogen bond network that preferentially stabilizes turns, which are known to be weak points upon thermal unfolding (Daggert and Levitt, 1993; Zhou et al., 1996). An increased number of hydrogen bonds that fix β-sheet A to the core of the molecule was observed in Fd_{Tl}, Fd_{Pf} and Fd_{Tm}. In contrast, however, to archaeal ferredoxins that mainly show an increased number of main chain

hydrogen bonds as consequence of the higher content of secondary structure, for Fd_{Tm} most of the additional hydrogen bonds involve side chains.

Current information on ferredoxins from hyperthermophilic organisms does not point out one single feature that plays a dominant role in protein hyperthermostability. This suggests that the type of interactions that increase thermostability may not be identical even within a single class of proteins.

4. High-potential iron–sulfur proteins

High-potential iron–sulfur proteins (HiPIPs) are a class of small proteins (62–85 amino acids) which contain a single [4Fe–4S]-cluster. Suggested functions of HiPIPs include electron transport in photosynthesis (Hochkoeppler et al., 1995; Schoepp et al., 1995), anaerobic metabolism (Bartsch, 1978), thiosulfate oxidation (Yamanaka and Fukumori, 1979) and iron oxidation (Kusano et al., 1992), although their exact metabolic role in bacteria is still unclear.

HiPIPs were identified in various strains of purple phototrophic bacteria including *Chromatium*, *Rhodocyclus*, *Thiocapsa* and *Ectothiorhodospira* and in the halophilic denitrifying bacterium *Paracoccus* sp. (Table 7). These proteins interconvert between the oxidation states $[4Fe–4S]^{3+}$ and $[4Fe–4S]^{2+}$ and show reduction potentials in the range from +500 to +50 mV (Mizrahi et al., 1980; Meyer et al., 1983; Przysiecki et al., 1985). Representatives with a high potential include the HiPIPs from *Chr. vinosum* (346 mV) and *Rhodospirillum salinarium* (500 mV) (Heering et al., 1995), while a lower potential is observed for HiPIP isoform I (120 mV) and isoform II (50 mV) from *E. halophila* (Tedro et al., 1985a).

HiPIPs show larger variations in their molecular sizes, amino acid sequences, net overall charges and redox potentials than observed for the low-potential ferredoxins (Bartsch, 1978; Meyer et al., 1983; Tedro et al., 1985a,b). Apart from the four cysteine ligands of the cluster (Cys43, 46, 63 and 77 according to the *Chr. vinosum* numbering scheme), Tyr19 and Gly75 are the only residues that are strictly conserved among all HiPIPs (Table 7).

Substitution of the cluster ligand Cys77 by serine in *Chr. vinosum* HiPIP resulted in formation of a stable cluster, while substitutions by alanine, aspartate and tyrosine resulted in a dramatic loss of stability (Agarwal et al., 1996). Both structure and reduction potential of the C77S mutant are almost identical to the wild-type, apart from the presence of a novel serine (O_γ) coordination of the iron–sulfur cluster (Bentrop et al., 1996a). Significant differences in the NMR (Babini et al., 1996) and EPR spectra are observed, however, for the oxidized C77S mutant compared to the wild-type, showing that differences in the electronic properties of the cluster may not necessarily correlate with structural differences.

Mutation of Tyr19 and the less well conserved aromatic residues Phe48 and Phe66 in *Chromatium vinosum* HiPIP revealed that aromatic residues play only a minor role in defining the electronic properties of the cluster (Soriano et al., 1996). However, mutation of Tyr19 showed that a replacement by smaller (Leu) or polar (His, Arg, Cys, Gln, Ser) amino acids results in decreased stability of the cluster, suggesting that Tyr19 plays a role for cluster stabilization by formation of a hydrophobic barrier, which excludes water from the cluster cavity (Agarwal et al., 1995; Li et al., 1996). Recent studies also proved the requirement of the

Table 7
Sequence alignment of high-potential iron-sulfur proteins (HiPIPs) from various organisms

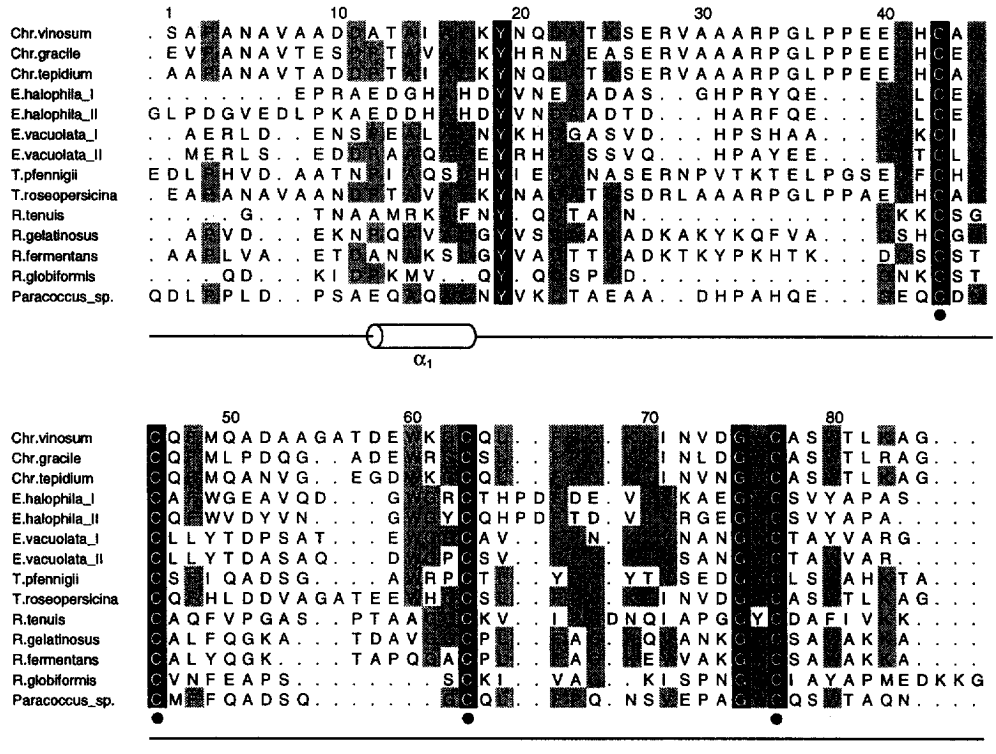

Sequence alignment of HiPIPs from *Chromatiom vinosum* (Tedro et al., 1981), *Chromatium gracile* (Tedro et al., 1981), *Chromatium tepidum* (Moulis et al., 1993), *Ectothiorhodospira halophila* isoform I and II (Tedro et al., 1985b), *Ectothiorhodospira vacuolata* isoform I and II (Ambler et al., 1994), *Thiocapsa pfennigii* (Tedro et al., 1974), *Thiocapsa roseopersicina* (Tedro et al., 1981), *Rhodocyclus tenuis* (Tedro et al., 1985a), *Rhodocyclus gelatinosus* (Tedro et al., 1976), *Rhodoferax fermentans* (van Driessche et al., 1997), *Rhodopila globiformis* (Ambler et al., 1993) and *Paracoccus* sp. (Tedro et al., 1977).
The *Chr. vinosum* numbering scheme is given at the top. The four cluster ligating cysteines are indicated by black circles (•). Strictly conserved residues at one position are highlighted by a black box and residues occurring with a frequency of ≥50% are marked by gray boxes. Elements of secondary structure present in the *Chr. vinosum* structure (Banci et al., 1995a) are given below the alignment.
The alignment was generated using the programs ClustalW (Higgins et al., 1992) and Alscript (Barton, 1993).

aromatic ring of Phe66 in *Chr. vinosum* necessary to maintain the stability of the iron–sulfur cluster in the oxidized state (Bian et al., 1996).

Similar results were obtained from extensive mutational analysis of the conserved Tyr12 in *E. halophila* HiPIP-I, revealing a significant destabilization of all mutant proteins (Iwagami et al., 1995). Although minor effects of the Y12F, Y12H and Y12W mutants on the redox potential (in the range of 17–22 mV) were reported, the principle function of the conserved

tyrosine is stabilization of the protein through hydrogen bonds involving its hydroxyl group and electrostatic interactions involving its aromatic ring (Iwagami et al., 1995). The low sequence similarity, however, poses some limitations on the generalization of this conclusion for the whole class of HiPIPs.

Similarities on the level of tertiary structure were deduced from the crystal structures of the oxidized HiPIPs from *Chromatium vinosum* (Carter et al., 1974; Freer et al., 1975), *Ectothiorhodospira halophila* (isoform-I) (Breiter et al., 1991), *Ectothiorhodospira vacuolata* (isoform-II) (Benning et al., 1994) and the reduced HiPIP from *Rhodocyclus tenuis* (Rayment et al., 1992).

In addition, the solution structure of reduced *E. halophila* HiPIP I (Bertini et al., 1994a, 1996a; Banci et al., 1994), which represents the first structure of a paramagnetic protein determined by NMR and of the reduced (Gaillard et al., 1992; Banci et al., 1995a) and oxidized (Nettesheim et al., 1992; Bertini et al., 1995c) HiPIP from *Chr. vinosum* are known.

The folding motif of all four HiPIPs is mainly characterized by a series of turns allowing the polypeptide chain to wrap around the iron–sulfur cluster (Fig. 4b). In *E. vacuolata* and *R. tenuis* water molecules have been identified that play an important role for stabilizing surface loops (Rayment et al., 1992; Benning et al., 1994). The only common element of secondary structure that is found in all but *E. halophila* HiPIP is an α-helix in the N-terminal part of the peptide chain.

The conserved Gly75 is located in close proximity to the conserved Tyr19 side chain in all structures known thus far (Fig. 4b). Gly75 is most probably conserved for steric reasons, because any side chain larger than Gly cannot easily be accommodated at this position (Rayment et al., 1992; Benning et al., 1994).

The orientation of additional aromatic residues in the proximity of the clusters varies between the different HiPIPs, but no correlation between the orientation of these residues and the cluster redox potential could be delineated (Benning et al., 1994).

The hydrogen bonding around the metal cluster and the geometry of the cluster itself is almost identical among the structurally characterized HiPIPs, showing that the number of hydrogen bonds is not a determinant of the redox potential for this protein class (Rayment et al., 1992). On the basis of this data one can conclude that the structural similarity of different HiPIPs (75–85% according to the definition of Rossman and Argos, 1975) is much higher than the sequence identities of approximately 30% (Benning et al., 1994).

A recent hypothesis draws a distinction between two groups of HiPIPs based on their redox potential: one group consists of the *Chromatium*-like HiPIPs with redox potentials of approximately 300–350 mV, modulated only by the solvation of the cluster. The second class is formed by the *Ectothiorhodospira*-like HiPIPs with potentials between 50 and 500 mV, modulated by the overall charge of the peptide and the solvation of the cluster (Heering et al., 1995).

A strong correlation between the net charge of HiPIPs and their reduction potential is also suggested from theoretical considerations (Banci et al., 1995b) and is confirmed from mutational studies of *E. halophila* HiPIP, in which Val68 of the cluster vicinity was replaced by Lys and Glu, respectively (Bertini et al., 1996b).

Attempts to investigate the electronic structure and electron transfer sites of the cluster and to correlate them with the molecular structure have been the focus of various NMR studies

(Nettesheim et al., 1983; Sola et al., 1989; Cowan and Sola, 1990; Bertini et al., 1991, 1997b; Banci et al., 1993a,b).

Comparison of the independently determined NMR solution structures of oxidized and reduced *Chr. vinosum* HiPIP shows only subtle conformational differences between the two redox states (Banci et al., 1995a; Bertini et al., 1995c) underlining the idea of a rigid structure for electron transfer proteins. In addition, no large differences are detected between the solid-state and solution structures, however, a detailed comparison is limited by the current resolution of both the crystal and the NMR structures (Bertini et al., 1995c).

4.1. The three-state hypothesis

Structural analysis proved the cluster geometry of *Chr. vinosum* HiPIP to be indistinguishable from that observed in the three-dimensional structure of the low-potential bacterial ferredoxin isolated from *Peptococcus aerogenes* (Adman et al., 1973, 1976). An attempt to reconcile these observations with the drastic differences in redox potentials led to the so-called 'three-state' hypothesis, proposed by Carter et al. (1972). According to this model, three oxidation states are available for the iron–sulfur cluster: $[4Fe–4S]^{3+}$, $[4Fe–4S]^{2+}$ and $[4Fe–4S]^{+}$. The HiPIPs exist in the $[4Fe–4S]^{3+}$ and $[4Fe–4S]^{2+}$ redox states, whereas low-potential ferredoxins exist in the $[4Fe–4S]^{+}$ and $[4Fe–4S]^{2+}$ state.

Factors likely to determine which oxidation states are available to the metal center when attached to a protein include the extent of hydrogen bonding to the cluster, location of the cysteine ligands, protein flexibility, solvent accessibility of the cluster, the number and positions of hydrophobic residues surrounding the metal center and the electrostatic field of the protein (Adman et al., 1975; Backes et al., 1991; Langen et al., 1992; Benning et al., 1994; Luchinat et al., 1994).

5. Concluding remarks

The rapid growth of structural data available on ferredoxins underlines the growing interest of many research groups in this area. The development of new and more sophisticated experimental techniques has allowed the isolation and characterization of a large number of new iron–sulfur proteins, revealing a much larger structural diversity than expected previously.

Surprising findings include the discovery of new cysteine patterns for cluster ligation (e.g. aldehyde oxido-reductase), non-cysteine cluster ligation (*P. furiousus* Fd), or structural variations in the protein moiety allowing an adaptation to extreme conditions (halophilic, acidophilic and hyperthermophilic Fd's) or to different functions (e.g. *Anabaena* heterocyst Fd).

In addition to the structure determination of wild-type ferredoxins, the application of site-directed mutagenesis has added a wealth of information to the understanding of structure–function relationships of these proteins: investigators are just beginning to discover the critical aspects of the peptide sequence which determine geometry, electronic properties and the redox potential of the iron–sulfur clusters. Progress has also been made towards understanding the critical forces influencing the specificity of electron transport and the electron-transfer reactivity.

In addition to those ferredoxins for which a three-dimensional structure is available and which have been focused on here, there is a still growing number of iron–sulfur proteins for which the cluster binding motif and the structure cannot readily be deduced from considerations of homologies. During recent years it has turned out that archaea are a particularly rich source of yet unknown ferredoxins. Since archaea constitute very ancient organisms, having diverged very early from other phyla, characterization of the corresponding ferredoxins may also be helpful for reaching a better understanding of the evolution of the early forms of life. In this context, one may expect that new structural motifs possibly related to yet unknown functions will be discovered in the near future.

Acknowledgements

We thank Professor Gerd N. La Mar and Dr. Detlef Bentrop for carefully reading the manuscript.

References

Adman, E.T., Sieker, L.C., Jensen, L.H., 1973 J. Biol. Chem. 248, 3987–3996.
Adman, E.T., Watenpaugh, K.D., Jensen, L.H., 1975 Proc. Natl. Acad. Sci. U.S.A. 72, 4854–4858.
Adman, E.T., Sieker, L.C., Jensen, L.H., 1976 J. Biol. Chem. 251, 3801–3806.
Agarwal, A., Li, D., Cowan, J.A., 1995 Proc. Natl. Acad. Sci. U.S.A. 92, 9440–9444.
Agarwal, A., Li, D., Cowan, J.A., 1996 J. Am. Chem. Soc. 118, 927–928.
Aketagawa, J., Tamura, G., 1980 Agric. Biol. Chem. 44, 2371–2378.
Alam, J., Whitaker, R.A., Krogmann, D.W., Curtis, S.E., 1986 J. Bacteriol. 168, 1265–1271.
Aliverti, A., Hagen, W.R., Zanetti, G., 1995 Fed. Eur. Biochem. Soc. Lett. 368, 220–224.
Ambler, R.P., Meyer, T.E., Kamen, M.D., 1993 Arch. Biochem. Biophys. 306, 215–222.
Ambler, R.P., Meyer, T.E., Kamen, M.D., 1994 Arch. Biochem. Biophys. 308, 78–81.
Aono, S., Bertini, I., Cowan, J.A., Luchinat, C., Rosato, A., Viezzoli, M.S., 1996 JBIC 1, 523–528.
Aono, S., Bentrop, D., Bertini, I., Luchinat, C., Macinai, R., 1997 Fed. Eur. Biochem. Soc. Lett. 412, 501–505.
Armengaud, J., Meyer, C., Jouanneau, Y., 1994 Biochem. J. 300, 413–418.
Armstrong, F.A., George, S.J., Thomson, A.J., Yates, M.G., 1988 Fed. Eur. Biochem. Soc. Lett. 234, 107–110.
Armstrong, F.A., George, S.J., Cammack, R., Hatchikian, E.C., Thomson, A.J., 1989 Biochem. J. 264, 265–274.
Babini, E., Bertini, I., Borsari, M., Capozzi, F., Dikiy, A., Eltis, L.D., Luchinat, C., 1996 J. Am. Chem. Soc. 118, 75–80.
Backes, G., Mino, Y., Loehr, T.M., Meyer, T.E., Cusanovich, M.A., Sweeney, W.V., Adman, E.T., Sanders-Loehr, J., 1991 J. Am. Chem. Soc. 113, 2055–2064.
Bacon, D.J., Anderson, W.F., 1988 J. Mol. Graphics 6, 219–220.
Banci, L., Bertini, I., Ciurli, S., Ferretti, S., Luchinat, C., Piccioli, M., 1993a Biochemistry 32, 9387–9397.
Banci, L., Bertini, I., Capozzi, F., Carloni, P., Ciurli, S., Luchinat, C., Piccioli, M., 1993b J. Am. Chem. Soc. 115, 3431–3440.
Banci, L., Bertini, I., Eltis, L.D., Felli, I.C., Kastrau, D.H.W., Luchinat, C., Piccoli, M., Piratelli, R., Smith, M., 1994 Eur. J. Biochem. 225, 715–725.
Banci, L., Bertini, I., Dikiy, A., Kastrau, D.H.W., Luchinat, C., Sompornpisut, P., 1995a Biochemistry 34, 206–219.
Banci, L., Bertini, I., Ciurli, S., Luchinat, C., Pierattelli, R., 1995b Inorg. Chim. Acta 240, 251–256.
Barata, B.A.S., Liang, J., Moura, I., LeGall, J., Moura, J.J.G., Huynh, B.H., 1992 Eur. J. Biochem. 204, 773–778.
Barton, G.J., 1993 Protein Eng. 6, 37–40.
Bartsch, R.G., 1978 Methods Enzymol. 53, 329–340.
Baumann, B., Sticht, H., Schärpf, M., Sutter, M., Haehnel, W., Rösch, P., 1996 Biochemistry 35, 12831–12841.
Beinert, H., 1990 FASEB J. 4, 2483–2491.
Beinert, H., Kennedy, M.C., 1993 FASEB J. 7, 1442–1449.
Beinert, H., Holm, R.H., Münck, E., 1997 Science 277, 653–659.

Benning, M.M., Meyer, T.E., Rayment, I., Holden, H.M., 1994 Biochemistry 33, 2476–2483.
Bentrop, D., Bertini, I., Capozzi, F., Dikiy, A., Eltis, L.D., Luchinat, C., 1996a Biochemistry 35, 5928–5936.
Bentrop, D., Bertini, I., Luchinat, C., Mendes, J., Piccioli, M., Teixeira, M., 1996b Eur. J. Biochem. 236, 92–99.
Bentrop, D., Bertini, I., Luchinat, C., Nitschke, W., Mühlenhoff, U., 1997 Biochemistry 36, 13629–13637.
Berg, J.M., Holm, R.H., 1982. In: Spiro, T.G. (Ed.), Iron-Sulfur Proteins. Wiley, New York, pp. 1–66.
Bertini, I., Briganti, F., Luchinat, C., Scozzafava, A., Sola, M., 1991 J. Am. Chem. Soc. 113, 1237–1245.
Bertini, I., Turano, P., Vila, A.J., 1993 Chem. Rev. 93, 2833–2932.
Bertini, I., Felli, I.C., Kastrau, D.H.W., Luchinat, C., Piccioli, M., Viezzoli, M.S., 1994a Eur. J. Biochem. 255, 703–714.
Bertini, I., Capozzi, F., Luchinat, C., Piccioli, M., Vila, A.J., 1994b J. Am. Chem. Soc. 116, 651–660.
Bertini, I., Donaire, A., Feinberg, B.A., Luchinat, C., Piccioli, M., Yuan, H., 1995a Eur. J. Biochem. 232, 192–205.
Bertini, I., Ciurli, S., Luchinat, C., 1995b. In: Clarke, M.J. (Ed.), Structure and Bonding, vol. 83. Springer Verlag, Berlin, pp. 1–54.
Bertini, I., Dikiy, A., Kastrau, D.H.W., Luchinat, C., Sompornpisut, P., 1995c Biochemistry 34, 9851–9858.
Bertini, I., Couture, M.M.J., Donaire, A., Eltis, L.D., Felli, I.C., Luchinat, C., Piccioli, M., Rosato, A., 1996a Eur. J. Biochem. 241, 440–452.
Bertini, I., Borsari, M., Bosi, M., Eltis, L.D., Felli, I.C., Luchinat, C., Piccioli, M., 1996b JBIC 1, 257–263.
Bertini, I., Luchinat, C., Rosato, A., 1996c Prog. Biophys. Mol. Biol. 66, 43–80.
Bertini, I., Dikiy, A., Luchinat, C., Macinai, R., Viezzoli, M.S., Vincenzini, M., 1997a Biochemistry 36, 3570–3579.
Bertini, I., Donaire, A., Felli, I.C., Luchinat, C., Rosato, A., 1997b Inorg. Chem. 36, 4798–4803.
Bian, S., Hemann, C.F., Hille, R., Cowan, J.A., 1996 Biochemistry 35, 14544–14552.
Blamey, J.M., Adams, M.W.W., 1994 Biochemistry 33, 1000–1007.
Böhme, H., Schrautemeier, B., 1987a Biochim. Biophys. Acta 891, 1–7.
Böhme, H., Schrautemeier, B., 1987b Biochim. Biophys. Acta 891, 115–120.
Breiter, D.R., Meyer, T.E., Rayment, I., Holden, H.M., 1991 J. Biol. Chem. 266, 18660–18667.
Breton, J.L., Duff, J.L.C., Butt, J.N., Armstrong, F.A., George, S.J., Pétillot, Y., Forest, E., Schäfer, G., Thomson, A.J., 1995 Eur. J. Biochem. 233, 937–946.
Bruschi, M., Guerlesquin, F., 1988 FEMS Microbiol. Rev. 54, 155–176.
Buckel, W., 1992 FEMS Microbiol. Rev. 88, 211–232.
Busse, S.C., La Mar, G.N., Howard, J.B., 1991 J. Biol. Chem. 266, 23714–23723.
Busse, S.C., La Mar, G.N., Yu, L.P., Howard, J.P., Smith, E.T., Zhou, Z.H., Adams, M.W.W., 1992 Biochemistry 31, 11952–11962.
Calzolai, L., Gorst, C.M., Zhou, Z.-H., Teng, Q., Adams, M.W.W., La Mar, G.N., 1995 Biochemistry 34, 11373–11384.
Calzolai, L., Zhou, Z.-H., Adams, M.W.W., La Mar, G.N., 1996 J. Am. Chem. Soc. 118, 2513–2514.
Calzolai, L., Gorst, C.M., Bren, K.L., Zhou, Z.-H., Adams, M.W.W., La Mar, G.N., 1997 J. Am. Chem. Soc. 119, 9341–9350.
Cammack, R., 1992 Adv. Inorg. Chem. 38, 281–322.
Cammack, R., Rao, K.K., Bargeron, C.P., Hutson, K.G., Andrew, P.W., Rogers, L.J., 1977a Biochem. J. 168, 205–209.
Cammack, R., Rao, K.K., Hall, D.O., Moura, J.J.G., Xavier, A.V., Bruschi, M., LeGall, J., Deville, A., Gayda, J.P., 1977b Biochim. Biophys. Acta 490, 311–321.
Carter, C.W., Kraut, J., Freer, S.T., Alden, R.A., Sieker, L.C., Adman, E., Jensen, L.H., 1972 Proc. Natl. Acad. Sci. U.S.A. 69, 3526–3529.
Carter, C.W., Kraut, J., Freer, S.T., Xuong, N.-H., Alden, R.A., Bartsch, R.G., 1974 J. Biol. Chem. 249, 4212–4225.
Chae, Y.K., Abildgaard, F., Moobery, E.S., Markley, J.L., 1994 Biochemistry 33, 3287–3295.
Chae, Y.K., Markley, J.L., 1995a Biochemistry 34, 188–193.
Chae, Y.K., Markley, J.L., 1995b. In: Mathies, P. (Ed.), Photosynthesis: from Light to Biosphere, vol. II. Kluwer Academic Publishers, Dordrecht/Boston/London, pp. 633–638.
Cheng, H., Markley, J.L., 1995 Annu. Rev. Biophys. Biomol. Struct. 24, 209–237.
Cheng, H., Xia, B., Reed, G.H., Markley, J.L., 1994 Biochemistry 33, 3155–3164.
Chitnis, P.R., Xu, Q., Chitnis, V.P., Nechushtai, R., 1995 Photosynth. Res. 44, 23–40.
Cooper, D.Y., Schleyer, H., Levin, S.S., Rosenthal, O., 1973 Ann. N. Y. Acad. Sci. 212, 227–247.
Correll, C.C., Batie, C.J., Ballou, D.P., Ludwig, M.L., 1992 Science 258, 1604–1610.
Cowan, J.A., Sola, M., 1990 Biochemistry 29, 5633–5637.
Cupp, J.R., Vickery, L.E., 1988 J. Biol. Chem. 263, 17418–17421.
Cushman, D.W., Tsai, R., Gunsales, I.C., 1967 Biochem. Biophys. Res. Commun. 26, 577–583.
Daggert, V., Levitt, M., 1993 J. Mol. Biol. 232, 600–619.
Darimont, B., Sterner, R., 1994 EMBO J. 13, 1772–1781.
Davies, M.D., Quin, L., Beck, J.L., Suslick, K.S., Koga, H., Horiuchi, T., Sligar, S.G., 1990 J. Am. Chem. Soc. 112, 7396–7398.
Davies, M.D., Sligar, S.G., 1992 Biochemistry 31, 11383–11389.
Davy, S.L., Osborne, M.J., Breton, J., Moore, G.R., Thomson, A.J., Bertini, I., Luchinat, C., 1995 Fed. Eur. Biochem. Soc. Lett. 363, 199–204.

de Pascalis, A.R., Schürmann, P., Bosshard, H.R., 1993 Fed. Eur. Biochem. Soc. Lett. 337, 217–220.
Donaire, A., Gorst, C.M., Zhou, Z.H., Adams, M.W.W., La Mar, G.N., 1994 J. Am. Chem. Soc. 116, 6841–6849.
Donaire, A., Zhou, Z.-H., Adams, M.W.W., La Mar, G.N., 1996 J. Biomolec. NMR 7, 35–47.
Duée, E.D., Fanchon, E., Vicat, J., Sieker, L.C., Meyer, J., Moulis, J.-M., 1994 J. Mol. Biol. 243, 683–695.
Dunn, P.P.J., Gray, J.C., 1988 Plant Mol. Biol. 11, 311–320.
Feinberg, B.A., Lo, X., Iwamoto, T., Tomich, J.M., 1997 Protein Eng. 10, 69–75.
Feinberg, B.A., Ryan, M.D., 1996. In: Lenaz, G., Milazzo, G. (Eds.), Comprehensive Textbook on Bioelectrochemistry, vol. 4. Birkhäuser Verlag, Basel, pp. 325–359.
Freer, S.T., Alden, R.A., Carter, C.W., Kraut, J., 1975 J. Biol. Chem. 250, 46–54.
Frolow, F., Harel, M., Sussman, J.L., Mevarech, M., Shoham, M., 1996 Nat. Struct. Biol. 3, 452–458.
Fujii, T., Hata, Y., Wagaki, T., Tanaka, N., Oshima, T., 1996 Nat. Struct. Biol. 3, 834–837.
Fujii, T., Hata, Y., Oozeki, M., Moriyama, H., Wagaki, T., Tanaka, N., Oshima, T., 1997 Biochemistry 36, 1505–1513.
Fujinaga, J., Gaillard, J., Meyer, J., 1993 Biochem. Biophys. Res. Commun. 194, 104–111.
Fukuyama, K., Hase, T., Matsumoto, S., Tsukihara, T., Katsube, Y., Tanaka, N., Kakudo, M., Wada, K., Matsubara, H., 1980 Nature 286, 522–524.
Fukuyama, K., Nagahara, Y., Tsukihara, T., Katsube, Y., Hase, T., Matsubara, H., 1988 J. Mol. Biol. 199, 183–193.
Fukuyama, K., Matsubara, H., Tsukihara, T., Katsube, Y., 1989 J. Mol. Biol. 210, 383–398.
Fukuyama, K., Ueki, N., Nakamura, H., Tsukihara, T., Matsubara, H., 1995 J. Biochem. 117, 1017–1023.
Gaillard, J., Albrand, J.-P., Moulis, J.-M., Wemmer, D.E., 1992 Biochemistry 31, 5632–5639.
Gaillard, J., Quinkal, I., Moulis, J.-M., 1993 Biochemistry 32, 9881–9887.
George, S.J., Richards, A.J.M., Thomson, A.J., Yates, M.G., 1989 Biochem. J. 264, 275–284.
Golinelli, M.P., Akin, L.A., Crouse, B.R., Johnson, M.K., Meyer, J., 1996 Biochemistry 35, 8995–9002.
Golinelli, M.P., Gognon, J., Meyer, J., 1997 Biochemistry 36, 11797–11803.
Gómez-Moreno, C., Medina, M., Hurley, J.K., Cusanovich, M.A., Markley, J.M., Cheng, H., Xia, B., Chae, Y.K., Tollin, G., 1994 Biochem. Soc. Trans. 22, 796–800.
Gorst, C.M., Yeh, Y.H., Teng, Q., Calzolai, L., Zhou, Z.H., Adams, M.W.W., La Mar, G.N., 1995a Biochemistry 34, 600–610.
Gorst, C.M., Zhou, Z.H., Ma, K., Teng, Q., Howard, J.B., Adams, M.W.W., La Mar, G.N., 1995b Biochemistry 34, 8788–8795.
Grabau, C., Schatt, E., Jouanneau, Y., Vignais, P.M., 1991 J. Biol. Chem. 266, 3294–3299.
Greenfield, N.J., Wu, X., Jordan, F., 1989 Biochim. Biophys. Acta 995, 246–254.
Hase, T., Wada, K., Matsubara, H., 1977a J. Biochem. 82, 277–286.
Hase, T., Matsubara, H., Evans, M.C.W., 1977b J. Biochem. 81, 1745–1749.
Hase, T., Wakabayashi, S., Matsubara, H., Kerscher, L., Oesterhelt, D., Rao, K.K., Hall, D.O., 1978 J. Biochem. 83, 1657–1670.
Hase, T., Matsubara, H., Ben-Amotz, A., Rao, K.K., Hall, D.O., 1980 Phytochemistry 19, 2065–2070.
Hase, T., Matsubara, H., Huber, G.N., Rogers, L.J., 1982 J. Biochem. 92, 1347–1356.
Hatanaka, H., Tanimura, R., Katoh, S., Inagaki, F., 1997 J. Mol. Biol. 268, 922–933.
Hayashida, N., Matsubayashi, T., Shinozaki, K., Sugiura, M., Inoue, K., Hiyama, T., 1987 Curr. Genet. 12, 247–250.
Heering, H.A., Bulsink, Y.B.M., Hagen, W.R., Meyer, T.E., 1995 Biochemistry 34, 14675–14686.
Higgins, D.G., Bleasby, A.J., Fuchs, R., 1992 Comput. Appl. Biosci. 8, 189–191.
Hintz, M.J., Mock, D.M., Peterson, L.L., Tuttle, K., Peterson, J.A., 1982 J. Biol. Chem. 257, 14324–14332.
Hochkoeppler, A., Ciurli, S., Venturoli, G., Zannoni, D., 1995 Fed. Eur. Biochem. Soc. Lett. 357, 70–74.
Hoj, P.B., Svendsen, I., Scheller, H.V., Moller, B.L., 1987 J. Biol. Chem. 262, 12676–12684.
Holden, H.M., Jacobson, B.L., Hurley, J.K., Tollin, G., Oh, B.H., Skjeldal, L., Chae, Y.K., Cheng, H., Xia, B., Markley, J.L., 1994 J. Bioenerg. Biomemb. 26, 67–88.
Howard, J.B., Lorsbach, T.W., Ghosh, D., Melis, K., Stout, C.D., 1983 J. Biol. Chem. 258, 508–522.
Huber, J.G., Gaillard, J., Moulis, J.M., 1995 Biochemistry 34, 194–205.
Huber, R., Hof, P., Duarte, R.O., Moura, J.J.G., Moura, I., Liu, M.-Y., LeGall, J., Hille, R., Archer, M., Roamao, M.J., 1996 Proc. Natl. Acad. Sci. U.S.A. 93, 8846–8851.
Hurley, J.K., Salamon, Z., Meyer, T.E., Fitch, J.C., Cusanovich, M.A., Markley, J.L., Cheng, H., Xia, B., Chae, Y.K., Medina, M., Gómez-Moreno, C., Tollin, G., 1993a Biochemistry 32, 9346–9354.
Hurley, J.K., Cheng, H., Xia, B., Markley, J.L., Medina, M., Gómez-Moreno, C., Tollin, G., 1993b J. Am. Chem. Soc. 115, 11698–11701.
Hurley, J.K., Caffrey, M.S., Markley, J.L., Cheng, H., Xia, B., Chae, Y.K., Holden, H.M., Tollin, G., 1995 Protein Sci. 4, 58–64.
Hurley, J.K., Fillat, M.F., Gómez-Moreno, C., Tollin, G., 1996a J. Am. Chem. Soc. 118, 5526–5531.
Hurley, J.K., Schmeits, J.L., Genzor, C., Gómez-Moreno, C., Tollin, G., 1996b Arch. Biochem. Biophys. 333, 243–250.
Hurley, J.K., Weber-Main, A.M., Stankovich, M.T., Benning, M.M., Thoden, J.B., Vanhooke, J.L., Holden, H.M., Chae, Y.K., Xia, B., Cheng, H., Markley, J.L., Martinez-Julvez, M., Gomez-Moreno, C., Schmeits, J.L., Tollin, G., 1997a Biochemistry 36, 11100–11117.

Hurley, J.K., Weber-Main, A.M., Hodges, A.E., Stankovich, M.T., Benning, M.M., Holden, H.M., Cheng, H., Xia, B., Markley, J.L., Genzor, C., Gomez-Moreno, C., Hafezi, R., Tollin, G., 1997b Biochemistry 36, 15109–15117.
Hutson, K.G., Rogers, L.J., 1975 Biochem. Soc. Trans. 3, 377–379.
Iametti, S., Uhlmann, H., Sala, N., Bernhardt, R., Ragg, E., Bonomi, F., 1996 Eur. J. Biochem. 239, 818–826.
Ichikawa, Y., Hamamoto, I., Waki, N., Iwahashi, K., Hiwatashi, A., Tsubaki, M., 1987. In: Matsubara, H., Katsube, Y., Wada, H. (Eds.), Iron–Sulfur Protein Research. Japan Scientific Societies Press, Tokyo/Springer Verlag, Berlin, pp. 97–105.
Ida, S., 1977 J. Biochem. 82, 915–918.
Iismaa, S.E., Vazquez, A.A., Jensen, G.M., Stephens, P.J., Butt, J.N., Armstrong, F.A., Burgess, B.K., 1991 J. Biol. Chem. 266, 21563–21571.
Ikemizu, S., Bando, M., Sato, T., Morimoto, Y., Tsukihara, T., 1994 Acta Crystallogr. D 50, 167–174.
Isas, J.M., Burgess, B.K., 1994 J. Biol. Chem. 269, 19404–19409.
Isas, J.M., Yannone, S.M., Burgess, B.K., 1994 J. Biol. Chem. 270, 21258–21263.
Iwagami, S.G., Creagh, A.L., Haynes, C.A., Borsari, M., Felli, I.C., Piccoli, M., Eltis, L.D., 1995 Protein Sci. 4, 2562–2572.
Iwasaki, T., Wagaki, T., Isogai, Y., Tanaka, K., Ilzuka, T., Oshima, T., 1994 J. Biol. Chem. 269, 29444–29450.
Iwasaki, T., Wagaki, T., Oshima, T., 1995 J. Biol. Chem. 270, 17878–17883.
Iwasaki, T., Suzuki, T., Kon, T., Imai, T., Urushiyama, A., Ohmori, D., Oshima, T., 1997 J. Biol. Chem. 272, 3453–3458.
Jacobson, B.L., Chae, Y.K., Markley, J.L., Rayment, I., Holden, H.M., 1993 Biochemistry 32, 6788–6793.
Jaenicke, R., 1991 Eur. J. Biochem. 202, 715–728.
Jensen, G.M., Warshel, A., Stephens, P.J., 1994 Biochemistry 33, 10911–10924.
Jouanneau, Y., Meyer, C., Gaillard, J., Vignais, P.M., 1990 Biochim. Biophys. Res. Commun. 171, 273–279.
Jouanneau, Y., Meyer, C., Gaillard, J., Forest, E., Gagnon, J., 1993 J. Biol. Chem. 268, 10636–10644.
Jouanneau, Y., Meyer, C., Naud, I., Klipp, W., 1995a Biochim. Biophys. Acta 1232, 33–42.
Jouanneau, Y., Hugo, N., Armengaud, J., Naud, I., Meyer, C., Willison, J.C., 1995b. In: Proc. of the Xth International Congress on Photosynthesis. Montpellier, France.
Kamlowski, A., van der Est, A., Fromme, P., Stehlik, D., 1997 Biochim. Biophys. Acta 1319, 185–198.
Kamo, M., Kotani, N., Tsugita, A., He, Y.K., Nozu, Y., 1989 Protein Seq. Data Anal. 2, 289–293.
Kazanis, S., Pochapsky, T.C., 1997 J. Biomolec. NMR 9, 337–346.
Kazanis, S., Pochapsky, T.C., Barnhart, T.M., Penner-Hahn, J.E., Mirza, U.A., Chait, B.T., 1995 J. Am. Chem. Soc. 117, 6625–6626.
Kemper, M.A., Stout, C.D., Lloyd, S.J., Prasad, G.S., Fawcett, S., Armstrong, F.A., Shen, B., Burgess, B.K., 1997 J. Biol. Chem. 272, 15620–15627.
Kerscher, L., Oesterhelt, D., 1976 Fed. Eur. Biochem. Soc. Lett. 67, 320–322.
Kerscher, L., Oesterhelt, D., 1977 Fed. Eur. Biochem. Soc. Lett. 83, 197–201.
Kerscher, L., Oesterhelt, D., Cammack, R., Hall, D.O., 1976 Eur. J. Biochem. 71, 101–107.
Kerscher, L., Nowitzki, S., Oesterhelt, D., 1982 Eur. J. Biochem. 128, 223–230.
Kisker, C., Schindlein, H., Rees, D.C., 1997 Annu. Rev. Biochem. 66, 233–267.
Kissinger, C.R., Sieker, L.C., Adman, E.T., Jensen, L.H., 1991 J. Mol. Biol. 219, 693–715.
Koike, H., Ikeuchi, M., Hiyama, T., Inoue, Y., 1989 Fed. Eur. Biochem. Soc. Lett. 253, 257–263.
Kraulis, P.K., 1991 J. Appl. Crystallogr. 24, 946–950.
Krauß, N., Schubert, W.-D., Klukas, O., Fromme, P., Witt, H.T., Saenger, W., 1996 Nat. Struct. Biol. 3, 965–973.
Kusano, T., Takeshima, T., Sugawara, K., Inoue, C., Shiratori, T., Yana, T., Fukumori, Y., Yamanaka, T., 1992 J. Biol. Chem. 267, 11242–11247.
Kyritsis, P., Huber, J.G., Quinkal, I., Gaillard, J., Moulis, J.-M., 1997 Biochemistry 36, 7839–7846.
Lambeth, J.D., Kamin, H., 1979 J. Biol. Chem. 254, 2766–2774.
Lambeth, J.D., Saybert, D.W., Lacaster, J.R., Salerno, J.C., Kamin, H., 1982 Mol. Cell. Biochem. 45, 13–31.
Langen, R., Jensen, G.M., Jacob, U., Stephens, P.J., Washel, A., 1992 J. Biol. Chem. 267, 25625–25627.
Lea, P.J., Miflin, B.J., 1984 Nature 251, 614–616.
Lelong, C., Sétif, P., Bottin, H., André, F., Neumann, J.-M., 1995 Biochemistry 34, 14462–14473.
Lelong, C., Boekema, E.J., Kruip, J., Bottin, H., Roegner, M., Sétif, P., 1996 EMBO J. 15, 2160–2168.
Li, D., Agarwal, A., Cowan, J.A., 1996 Inorg. Chem. 35, 1121–1125.
Lipscomb, J.D., Sligar, S.G., Namtvedt, M.J., Gunsalus, I.C., 1976 J. Biol. Chem. 251, 1116–1124.
Luchinat, C., Capozzi, F., Borsari, M., Battistuzzi, G., Sola, M., 1994 Biochem. Biophys. Res. Commun. 203, 436–442.
Lyons, T.A., Ratnaswamy, G., Pochapsky, T.C., 1996 Protein Sci. 5, 627–639.
Macedo, A.L., Moura, I., Surerus, K.K., Papaefthymiou, V., Liu, M.Y., LeGall, J., Munck, E., Moura, J.J.G., 1994 J. Biol. Chem. 269, 8052–8058.
Macedo-Ribeiro, S., Darimont, B., Sterner, R., Huber, R., 1996 Structure 4, 1291–1301.
Macedo-Ribeiro, S., Darimont, B., Sterner, R., 1997 Biol. Chem. 378, 331–338.
Martin, A.E., Burgess, B.K., Iismaa, S.E., Smartt, C.T., Jacobson, M.R., Dean, D.R., 1989 J. Bacteriol. 171, 3162–3167.

Martin, A.E., Burgess, B.K., Stout, C.D., Cash, V.C., Dean, D.R., Jensen, G.M., Stephens, P.J., 1990 Proc. Natl. Acad. Sci. U.S.A. 87, 598–602.
Masaki, R., Yoshikawa, S., Matsubara, H., 1982 Biochim. Biophys. Acta 700, 101–109.
Mason, J.I., Boyd, G.S., 1971 Eur. J. Biochem. 21, 308–321.
Matsubara, H., Hase, T., Wakabayashi, S., Wada, K., 1978. In: Matsubara, H., Yamanaka, T. (Eds.), Evolution of Protein Molecules. Japan Sci. Soc. Press, Tokyo, pp. 209–237.
Matsubara, H., Hase, T., Wakabayashi, S., Wada, K., 1980. In: Sigman, D.S., Brazier, M.A.B. (Eds.), The Evolution of Protein Structure and Function. Academic Press, New York, pp. 245–266.
Matsubara, H., Hase, T., 1983. In: Jensen, U., Fairbrothers, D.E. (Eds.), Proteins and Nucleic Acids in Plant Systematics. Springer-Verlag, Berlin, pp. 168–181.
Matsubara, H., Saeki, K., 1992 Adv. Inorg. Chem. 38, 223–280.
Merritt, E.A., Stout, G.H., Turley, S., Sieker, L.C., Jensen, L.H., Orme-Johnson, W.H., 1993 Acta Cryst. D 49, 272–281.
Merritt, E.A., Murphy, M., 1994 Acta Cryst. D 50, 869–873.
Meyer, J., 1988 Trends Ecol. Evol. 3, 222–226.
Meyer, J., 1993 Biochim. Biophys. Acta 1174, 108–110.
Meyer, J., Bruschi, M.H., Bonicel, J.J., Bovier-Lapierre, G.E., 1986 Biochemistry 25, 6054–6061.
Meyer, J., Moulis, J.-M., Scherrer, N., Gagnon, J., Ulrich, J., 1993 Biochem. J. 294, 622–623.
Meyer, J., Fujinaga, J., Gaillard, J., Lutz, M., 1994 Biochemistry 33, 13642–13650.
Meyer, T.E., Cusanovich, M.A., 1989 Biochim. Biophys. Acta 975, 1–28.
Meyer, T.E., Przysiecki, C.T., Watkins, J.A., Bhattacharyya, A., Simondsen, R.P., Cusanovich, M.A., Tollin, G., 1983 Proc. Natl. Acad. Sci. U.S.A. 80, 6740–6744.
Minami, Y., Wakabayashi, S., Wada, K., Matsubara, H., Kerscher, L., Oesterhelt, D., 1985 J. Biochem. 97, 745–753.
Miura, S., Tomita, S., Ichikawa, Y., 1991 J. Biol. Chem. 266, 19212–19216.
Mizrahi, I.A., Meyer, T.E., Cusanovich, M.A., 1980 Biochemistry 19, 4727–4733.
Morgan, T.V., Stephens, P.J., Devlin, F., Stout, C.D., Melis, K.A., Burgess, B.K., 1984 Proc. Natl. Acad. Sci. U.S.A. 81, 1931–1935.
Mortenson, L.E., Valentine, R.C., Carnahan, J.E., 1962 Biochem. Biophys. Res. Commun. 7, 448–452.
Moshiri, F., Kim, J.W., Fu, C., Maier, R.J., 1994 Mol. Microbiol. 14, 101–114.
Moulis, J.-M., 1996 Biochim. Biophys. Acta 1308, 12–14.
Moulis, J.-M., Scherrer, N., Gagnon, J., Forest, E., Petillot, Y., Garcia, D., 1993 Arch. Biochem. Biophys. 305, 186–192.
Moulis, J.-M., Davasse, V., 1995 Biochemistry 34, 16781–16788.
Moulis, J.-M., Sieker, L.C., Wilson, K.S., Dauter, Z., 1996a Protein Sci. 5, 1765–1775.
Moulis, J.-M., Davasse, V., Golinelli, M.-P., Meyer, J., Quinkal, I., 1996b JBIC 1, 2–14.
Moura, J.J.G., Moura, I., Kent, T.A., Lipscomb, J.D., Huynh, B.H., LeGall, J., Xavier, A.V., Munck, E., 1982 J. Biol. Chem. 257, 6259–6267.
Naud, I., Vinçon, M., Garin, J., Gaillard, J., Forest, E., Jouanneau, Y., 1994 Eur. J. Biochem. 222, 933–939.
Naud, I., Meyer, C., David, L., Breton, J., Gaillard, J., Jouanneau, Y., 1996 Eur. J. Biochem. 237, 399–405.
Navarro, J.A., Hervás, M., Genzor, C.G., Cheddar, G., Fillat, M.F., de la Rosa, M.A., Gómez-Moreno, C., Cheng, H., Xia, B., Chae, Y.K., Yan, H., Wong, B., Straus, N.A., Markley, J.L., Hurley, J.K., Tollin, G., 1995 Arch. Biochem. Biophys. 321, 229–238.
Nettesheim, D.G., Meyer, T.E., Feinberg, B.A., Otvos, J.D., 1983 J. Biol. Chem. 258, 8235–8239.
Nettesheim, D.G., Harder, S.R., Feinberg, B.A., Otvos, J.D., 1992 Biochemistry 31, 1234–1244.
Ogata, M., Kondo, S., Okawara, N., Yagi, T., 1988 J. Biochem. 103, 121–125.
Oh, B.H., Markley, J.L., 1990a Biochemistry 29, 3993–4004.
Oh, B.H., Markley, J.L., 1990b Biochemistry 29, 4012–4017.
Oh, B.H., Mooberry, E.S., Markley, J.L., 1990 Biochemistry 29, 4004–4011.
Oh-oka, H., Takahashi, Y., Kuriyama, K., Saeki, K., Matsubara, H., 1988 J. Biochem. 103, 962–968.
Ohyama, K., Fukzawa, H., Kohchi, T., Shirai, H., Sano, T., Umesono, K., Shiki, Y., Takeuchi, M., Chang, Z., Aota, S., Inokuchi, H., Ozeki, H., 1986 Nature 322, 572–574.
Pfeifer, F., Griffig, J., Oesterhelt, D., 1993 Mol. Gen. Genet. 239, 66–71.
Pfeil, W., Gesierich, U., Kleemann, G.R., Sterner, R., 1997 J. Mol. Biol. 272, 591–596.
Piubelli, L., Aliverti, A., Bellintani, F., Zanetti, G., 1996 Eur. J. Biochem. 236, 465–469.
Pochapsky, T.C., Ye, X.M., Ratnaswamy, G., Lyons, T.A., 1994a Biochemistry 33, 6424–6432.
Pochapsky, T.C., Ratnaswamy, G., Patera, A., 1994b Biochemistry 33, 6433–6441.
Pochapsky, T.C., Lyons, T.A., Kazanis, S., Arakaki, T., Ratnaswamy, G., 1996 Biochimie 78, 723–733.
Przysiecki, C.T., Meyer, T.E., Cusanovich, M.A., 1985 Biochemistry 24, 2542–2549.
Quinkal, I., Davasse, V., Gaillard, J., Moulis, J.-M., 1994 Protein Eng. 7, 681–687.
Quinkal, I., Kyritsis, P., Kohzuma, T., Im, S.-C., Sykes, A.G., Moulis, J.-M., 1996 Biochim. Biophys. Acta 1295, 201–208.
Ratnaswamy, G., Pochapsky, T.C., 1993 Magn. Reson. Chem. 31, 73–77.

Rayment, I., Wesenberg, G., Meyer, T.E., Cusanovich, M.A., Holden, H.M., 1992 J. Mol. Biol. 228, 672–686.
Rees, D.C., Adams, M.W.W., 1995 Structure 3, 251–254.
Romao, M.J., Archer, M., Moura, I., Moura, J.J.G., LeGall, J., Engh, R., Schneider, M., Hof, P., Huber, R., 1995 Science 270, 1170–1176.
Rossman, M.G., Argos, P., 1975 J. Biol. Chem. 250, 7525–7532.
Rouault, T.A., Klausner, R.D., 1996 Trends Biochem. Sci. 21, 174–177.
Rousseau, F., Lagoutte, B., 1993 EMBO J. 12, 1755–1765.
Rypniewski, W.R., Breiter, D.R., Benning, M.M., Wesenberg, G., Oh, B., Markley, J.L., Rayment, I., Holden, H.M., 1991 Biochemistry 30, 4126–4131.
Saeki, K., Suetsugu, Y., Tokuda, K.I., Miyatake, Y., Young, D.A., Marrs, B.L., Matsubara, H., 1991 J. Biol. Chem. 266, 12889–12895.
Saeki, K., Tokuda, K.I., Fukuyama, K., Matsubara, H., Nadanami, K., Go, M., Itoh, S., 1996 J. Biol. Chem. 271, 31399–31406.
Salamon, Z., Tollin, G., 1992 Bioelectrochem. Bioenerg. 27, 381–391.
Schäfer, G., Purschke, W., Schmidt, C.L., 1996 Fed. Eur. Microbiol. Soc. Microbiol. Rev. 18, 173–188.
Schantz, R., Bogorad, L., 1988 Plant Mol. Biol. 11, 239–248.
Schmidt, H., Heinz, E., 1990 Plant Physiol. 94, 214–220.
Schoepp, B., Parot, P., Menin, L., Gaillard, J., Richaud, P., Vermeglio, A., 1995 Biochemistry 34, 11736–11742.
Schrautemeier, B., Böhme, H., 1985 Fed. Eur. Biochem. Soc. Lett. 184, 304–308.
Schübel, U., Kraut, M., Mörsdorf, G., Meyer, O., 1995 J. Bacteriol. 177, 2197–2203.
Séry, A., Housset, D., Serre, L., Bonicel, J., Hatchikian, C., Frey, M., Roth, M., 1994 Biochemistry 33, 15408–15417.
Shen, B., Martin, L.L., Butt, J.N., Armstrong, F.A., Stout, C.D., Jensen, G.M., Stephens, P.J., La Mar, G.N., Gorst, C.M., Burgess, B.K., 1993 J. Biol. Chem. 268, 25928–25939.
Shen, B., Jollie, D.R., Stout, C.D., Diller, T.C., Armstrong, F.A., Gorst, C.M., La Mar, G.N., Stephens, P.J., Burgess, B.K., 1994 J. Biol. Chem. 269, 8564–8575.
Shen, B., Jollie, D.R., Diller, T.C., Stout, C.D., Stephens, P.J., Burgess, B.K., 1995 Proc. Natl. Acad. Sci. U.S.A. 92, 10064–10068.
Shergill, J.K., Golinelli, M.-P., Cammack, R., Meyer, J., 1996 Biochemistry 35, 12842–12848.
Shiro, V., Ilzuka, T., Makino, R., Ishimura, Y., Morishima, I., 1989 J. Am. Chem. Soc. 111, 7707–7711.
Simpson, E.R., Miller, D.A., 1978 Arch. Biochem. Biophys. 190, 800–808.
Skjeldal, L., Markley, J.L., Coghlan, V.M., Vickery, L.E., 1991 Biochemistry 30, 9078–9083.
Sligar, S.G., Gunsalus, I.C., 1976 Proc. Natl. Acad. Sci. U.S.A. 73, 1078–1082.
Smith, E.T., Feinberg, B.A., 1990 J. Biol. Chem. 265, 14371–14376.
Smith, E.T., Richards, J.H., Tomich, J.M., Feinberg, B.A., 1991a J. Am. Chem. Soc. 113, 688–689.
Smith, E.T., Tomich, J.M., Iwamoto, T., Richards, J.H., Mao, Y., Feinberg, B.A., 1991b Biochemistry 30, 11669–11676.
Smith, E.T., Bennet, D.W., Feinberg, B.A., 1991c Anal. Chim. Acta 251, 27–33.
Smith, E.T., Blamey, J.M., Zhou, Z.H., Adams, M.W.W., 1995 Biochemistry 34, 7161–7169.
Sola, M., Cowan, J.A., Gray, H.B., 1989 J. Am. Chem. Soc. 111, 6627–6630.
Soman, J., Iismaa, S., Stout, C.D., 1991 J. Biol. Chem. 266, 21558–21562.
Soriano, A., Li, D., Bian, S., Agarwal, A., Cowan, J.A., 1996 Biochemistry 35, 12479–12486.
Sticht, H., Wildegger, G., Bentrop, D., Darimont, B., Sterner, R., Rösch, P., 1996 Eur. J. Biochem. 237, 726–735.
Stout, C.D., 1989 J. Mol. Biol. 205, 545–555.
Stout, C.D., 1993 J. Biol. Chem. 268, 25920–25927.
Tagawa, K., Arnon, D.I., 1962 Nature 195, 537–543.
Takahashi, Y., Hase, T., Wada, K., Matsubara, H., 1983 Plant Cell Physiol. 24, 189–198.
Tanaka, M., Nakashima, T., Benson, A.M., Mower, H.F., Yasunobu, K.T., 1966 Biochemistry 5, 1666–1680.
Tanaka, M., Haniu, M., Yasunobu, K.T., Rao, K.K., Hall, D.O., 1976 Biochem. Biophys. Res. Commun. 69, 759–765.
Tedro, S.M., Meyer, T.E., Kamen, M.D., 1974 J. Biol. Chem. 249, 1182–1188.
Tedro, S.M., Meyer, T.E., Kamen, M.D., 1976 J. Biol. Chem. 251, 129–136.
Tedro, S.M., Meyer, T.E., Kamen, M.D., 1977 J. Biol. Chem. 252, 7826–7833.
Tedro, S.M., Meyer, T.E., Bartsch, R.G., Kamen, M.D., 1981 J. Biol. Chem. 256, 731–735.
Tedro, S.M., Meyer, T.E., Kamen, M.D., 1985a Arch. Biochem. Biophys. 239, 94–101.
Tedro, S.M., Meyer, T.E., Kamen, M.D., 1985b Arch. Biochem. Biophys. 241, 656–664.
Teixeira, M., Batista, R., Campos, A.P., Gomes, C., Mendes, J., Pacheo, I., Anemüller, S., Hagen, W.R., 1995 Eur. J. Biochem. 227, 322–327.
Teng, Q., Zhou, Z.H., Smith, E.T., Busse, S.C., Howard, J.B., Adams, M.W.W., La Mar, G.N., 1994 Biochemistry 33, 6316–6326.
Thoenes, U., Flores, O.L., Neves, A., Devreese, B., van Beeumer, J.J., Huber, R., Romao, M.J., LeGall, J., Moura, J.J.G., Rodrigues-Posada, C., 1994 Eur. J. Biochem. 220, 901–910.
Tranqui, D., Jesoir, J.C., 1995 Acta Cryst. D 51, 155–159.

Trower, M.K., Marshall, J.E., Doleman, M.S., Emptage, M.H., Sariaslani, F.S., 1990 Biochim. Biophys. Acta 1037, 290–296.
Tsukihara, T., Fukuyama, K., Nakamura, M., Katsube, Y., Tanaka, N., Kakudo, M., Wada, K., Hase, T., Matsubara, H., 1981 Biochem. J. 90, 1763–1773.
Tsukihara, T., Fukuyama, K., Mizushima, M., Harioka, T., Kusoniki, M., Katsube, Y., Hase, T., Matsubara, H., 1990 J. Mol. Biol. 216, 399–410.
Tsutsui, T., Tsukihara, T., Fukuyama, K., Katsube, Y., Hase, T., Matsubara, H., Nishikawa, Y., Tanaka, N., 1983 J. Biochem. 94, 299–302.
van Driessche, G., Ciurli, S., Hochkoeppler, A., van Beeumen, J.J., 1997 Eur. J. Biochem. 244, 371–377.
Wakabayashi, S., Hase, T., Wada, K., Matsubara, H., Suzuki, K., Takaichi, S., 1978 J. Biochem. 83, 1305–1319.
Wakabayashi, S., Fujimoto, N., Wada, K., Matsubara, H., Kerscher, L., Oesterhelt, D., 1983 Fed. Eur. Biochem. Soc. Lett. 162, 21–24.
Wang, P.-L., Donaire, A., Zhou, Z.-H., Adams, M.W.W., La Mar, G.N., 1996 Biochemistry 35, 11319–11329.
Werber, M.M., Mevarech, M., 1978a Arch. Biochem. Biophys. 187, 447–456.
Werber, M.M., Mevarech, M., 1978b Arch. Biochem. Biophys. 186, 60–65.
Wildegger, G., Bentrop, D., Ejchart, A., Alber, M., Hage, A., Sterner, R., Rösch, P., 1995 Eur. J. Biochem. 229, 658–668.
Xia, B., Cheng, H., Skjeldal, L., Coghlan, V.M., Vickery, L.E., Markley, J.L., 1995 Biochemistry 34, 180–187.
Xia, B., Cheng, H., Bandarian, V., Reed, G.H., Markley, J.L., 1996 Biochemistry 35, 9488–9495.
Yamanaka, T., Fukumori, Y., 1979 Abstr. Annu. Meet. Am. Soc. Microbiol. 79, 117.
Ye, X.M., Pochapsky, T.C., Pochapsky, S.S., 1992 Biochemistry 31, 1961–1968.
Yoch, D.C., Carithers, R.P., 1979 Microbiol. Rev. 43, 384–421.
Zheng, L., Dean, D.R., 1994 J. Biol. Chem. 269, 18723–18726.
Zhou, H.X., Hoess, R.H., DeGrado, W.F., 1996 Nat. Struct. Biol. 3, 446–451.